

SMITH PREDICTOR BASED CONTROLLER DESIGN FOR A FLEXIBLE ROBOT ARM

A THESIS

SUBMITTED TO THE DEPARTMENT OF ELECTRICAL AND
ELECTRONICS ENGINEERING

AND THE GRADUATE SCHOOL OF ENGINEERING AND SCIENCE
OF BILKENT UNIVERSITY

IN PARTIAL FULFILLMENT OF THE REQUIREMENTS
FOR THE DEGREE OF
MASTER OF SCIENCE

By

Uğur Taşdelen

July, 2013

I certify that I have read this thesis and that in my opinion it is fully adequate, in scope and in quality, as a thesis for the degree of Master of Science.

Prof. Dr. Hitay Özbay(Advisor)

I certify that I have read this thesis and that in my opinion it is fully adequate, in scope and in quality, as a thesis for the degree of Master of Science.

Prof. Dr. Arif Bülent Özgüler (Co-Advisor)

I certify that I have read this thesis and that in my opinion it is fully adequate, in scope and in quality, as a thesis for the degree of Master of Science.

Prof. Dr. Ömer Morgül

I certify that I have read this thesis and that in my opinion it is fully adequate, in scope and in quality, as a thesis for the degree of Master of Science.

Assist. Prof. Dr. Melih Çakmakçı

Approved for the Graduate School of Engineering and Science:

Prof. Dr. Levent Onural
Director of the Graduate School

ABSTRACT

SMITH PREDICTOR BASED CONTROLLER DESIGN FOR A FLEXIBLE ROBOT ARM

Uğur Taşdelen

M.S. in Electrical and Electronics Engineering

Supervisor: Prof. Dr. Hitay Özbay

July, 2013

In this thesis, a new Smith predictor based controller is proposed for a flexible robot arm. A typical robot arm model includes high order modes with integral action from torque input to velocity output. Here we can also consider the effect of possible delays between the plant and the controller. The controller structure considered has an extended Smith predictor form. The designs use controller parametrization for stability and they also achieve certain performance objectives via interpolation conditions based on the disturbance rejection and setpoint tracking properties. This parametrization method allows widest freedom in controller parameters and this results in improved performance, both in set-point response and disturbance rejection. Free parameters in the controller determines the location of closed-loop poles. A hierarchical structure is used to extend Smith predictor structure to the position control loop. By protecting proposed structure, different approaches are shown to control the position. Compared to existing Smith predictor based designs, disturbance attenuation property with respect to periodic disturbances at a known frequency is improved. A two-degree of freedom controller structure is shown to be helpful in shaping the transient response under constant reference inputs. Stability robustness properties of this system are also investigated. Simulation results demonstrate the effectiveness of the proposed controller.

Keywords: Time Delay Systems, Flexible Robot Arm, Smith Predictor Based Controller, Robust Controller, Periodic Disturbance.

ÖZET

ESNEK BİR ROBOT KOLU İÇİN SMITH KESTİRİM TABANLI DENETLEYİCİ TASARIMI

Uğur Taşdelen

Elektrik ve Elektronik Mühendisliği Bölümü, Yüksek Lisans

Tez Yöneticisi: Prof. Dr. Hitay Özbay

Temmuz, 2013

Bu tezde, esnek robot kolları için Smith kestirim tabanlı denetleyici yapısında yeni bir denetleyici önerilmiştir. Girdi olarak tork ve çıktı olarak hız alındığında tipik bir robot kolu modeli integrator ile birlikte esnek modları içermektedir. Ayrıca denetleyici ve tesis arasındaki zaman gecikmesinin etkileride kaçınılmazdır. Bu tarz bir modelin kontrolü için önerilen denetleyici yapısı, Smith kestirimli yapının genişletilmiş şeklidir. Yapılan tasarımların kararlılığı kontrolör parametrizasyonu ile garanti altına alınmıştır ve bozucu etki regülasyonu ile basamak tepkisi gibi performans objektiflerinin gerçekleşmesi için bir takım interpolasyon şartlarının sağlanması yoluna gidilmiştir. Kullanılan parametrizasyon yöntemi denetleyici parametrelerinin seçiminde serbestlik sağlamıştır ve bu, bozucu etki regülasyonu ile basamak tepkisi gibi performans objektiflerinin iyi sonuçlar vermesinin önünü açmıştır. Belirtilen serbest parametreler kapalı döngü kutuplarının yerlerini belirlemektedir. Ayrıca, pozisyon kontrol döngüsü içinde hiyerarşik bir yapı kullanılmıştır. Önerilen yapıyı koruyarak farklı tasarımlar konum kontrolünde de kullanılmıştır. Önceden var olan diğer Smith kestirim tabanlı denetleyicilere göre özellikle frekansı bilinen sinüsoidal bozucu etki bastırımında gelişmeler kaydedilmiştir. Kullanılan iki-dereceli denetleyici yapısı, basamak referans istekleri için geçici hal etkisinin geliştirilmesinde avantajlar elde edilmesini sağlamıştır. Gürbüz kararlılık testleri de yapılmıştır. Elde edilen sonuçlar önerilen denetleyici yapısının kullanılabilirliğini ortaya koymuştur.

Anahtar sözcükler: Zaman Gecikmeli Sistemler, Esnek Robot Kolu, Smith Kestirim Tabanlı Denetleyici, Grbz Denetleyici, Periyodik Bozucu Etki.

Acknowledgement

I would like to express my sincere gratitude to Prof. Dr. Hitay Özbay for his supervision, guidance, suggestions, and encouragement throughout my graduate studies.

I would also like to thank Prof. Dr. Arif Bülent Özgüler and Prof. Dr. Ömer Morgül for their enlightening guidance in the development of the thesis.

I am also indebted to Assist. Prof. Dr. Melih Çakmakçı for reading and commenting on the thesis.

I would like to express my deepest appreciation to Evrim Onur Arı and Onur Cem Erdoğan for discussion on physical motivation behind the problem studied and their willingness to implement the ideas presented in the thesis on an experimental platform at ASELSAN Inc.

I express my special thanks to TÜBİTAK for their financial support.

Finally, I would like to express my appreciation to my family for their endless support throughout my life.

Contents

1	INTRODUCTION	1
2	SMITH PREDICTOR BASED CONTROL OF THE ROBOT ARM	10
2.1	Preliminaries	10
2.2	Plant Structure	12
2.3	Smith Predictor Based Controller Design for Velocity Control . .	13
2.3.1	Smith Predictor Based Controller for Constant Disturbance Rejection	15
2.3.2	Smith Predictor Based Controller Rejecting Constant and Ramp Disturbances	16
2.3.3	Smith Predictor Design To Reject Constant and Sinusoidal Disturbance	18
2.3.4	Smith Predictor Design To Reject Constant, Ramp and Si- nusoidal Disturbance	20
2.4	Pade Approximation of Time Delay for Controller Implementation	21
2.5	The Effects of Reference Filter	23

2.6	Smith Predictor Design For Position Control	25
2.6.1	Direct Approach To Plant	26
2.6.2	Indirect Approach To Plant	28
3	SIMULATIONS AND RESULTS	30
3.1	Different Designs for Velocity Control	31
3.2	Performance Analysis	32
3.2.1	Setpoint Response Analysis	32
3.2.2	Disturbance Rejection	34
3.3	Stability Robustness Analysis	35
3.4	Examples For Position Control	41
4	CONCLUSIONS	45

List of Figures

1.1	<i>Block diagram of a feedback system whose controller is in a Smith predictor structure</i>	3
1.2	<i>Equivalent block diagram of Smith predictor in terms of the transfer function from input to output</i>	4
1.3	<i>A representation of a flexible robot arm</i>	5
1.4	<i>Velocity control system for a robot arm</i>	6
2.1	<i>Closed-loop feedback system</i>	12
2.2	<i>Proposed Smith Predictor Based Controller Structure</i>	14
2.3	<i>Step response comparison for $T_d = 0.2$</i>	22
2.4	<i>Unit step response of a closed loop system for different cut-off frequencies</i>	24
2.5	<i>Hierarchical control structure for position control</i>	25
2.6	<i>Direct approach for position control</i>	26
2.7	<i>Indirect approach for position control</i>	29

3.1	<i>The alternative Smith predictor based controller of Matausek and Micic</i>	30
3.2	<i>Setpoint Responses</i>	33
3.3	<i>Corresponding torque demands</i>	33
3.4	<i>Disturbance Rejection Property of The Controllers</i>	34
3.5	<i>Nyquist Graph For The Design in Section 2.3.2</i>	36
3.6	<i>Nyquist Graph For The Design in Section 2.3.3</i>	37
3.7	<i>Vector Margin For Different K and T_d</i>	38
3.8	<i>Corresponding Step Responses</i>	39
3.9	<i>Corresponding Disturbance Rejection Properties</i>	39
3.10	<i>Illustration of Robust Stability</i>	40
3.11	<i>Unit step response for direct approach</i>	42
3.12	<i>Unit step response for indirect approach</i>	42
3.13	<i>Unit step response for %20 deviation on time delay T_d</i>	43
3.14	<i>Unit step response for %20 perturbation on the parameters of flexible modes</i>	44

List of Tables

1.1	Notation	9
2.1	Obtained controllers via second order Pade approximation of the delay	23
3.1	Stability Margins of The Designs	37

Chapter 1

INTRODUCTION

Time delay very often appears in many systems, such as electric, chemical processes, biological systems, communication networks, robotics, etc. When information or energy is transported from one location to another, time delay emerges depending on transmission, communication, computation and measurement lags and analysis time. The input-output relationship of a time delay system is given as

$$y(t) = u(t - T_d)$$

The transfer function of time delay element is given by $e^{-T_d s}$ which is not a rational function.

The delay in control action is called *transport delay* or *dead time*. Since a feedback system with transport delay in the loop is a special case of infinite dimensional systems having infinitely many poles, the appearance of dead time makes the system analysis and controller design more complicated. Classical controllers operate to make an action for a situation which emerged some time ago. The effects of dead time in control applications can be listed as below:

- Existence of time delay adds additional phase drop proportional to frequency.
- It may result in reducing system performance, or even cause instability.

- Typically, stability margins of the closed loop system declines with increasing delay.
- Time delay introduces infinitely many poles to the characteristic equation of the closed loop transfer function, hence makes the analysis difficult.

As a consequence, the issue of robustness, performance, controllability, observability and pole placement for these types of systems has attracted the attention of many scientists and researchers. Under some special cases, additional time delays in the feedback loop may improve stability and performance measures, [21]. But this is not the case for systems we consider in this thesis. In most of control applications with or without time delay, classical PID type controllers are still used, [2]. However, PID controllers are not so efficient if there is long time delay in process dynamics. Although derivative action of PID controllers is used for prediction purposes, it is not convenient for the structures with long dead time. Other predictive type of controllers are necessary to control a model with transport delay in an effective way. In 1957, Smith, [22], presented a particular controller structure in which the closed loop transfer function can be formed by designing a controller as if the process is delay free. This structure employs a feedback loop inside the controller. When there is long time delay, it is not possible to get sufficient information from output signal for prediction. Hence, prediction is established on control input in this structure. Transfer functions and parameters estimated from the plant are used in the feedback loop. The structure of Smith predictor based controller is shown in Figure 1.1.

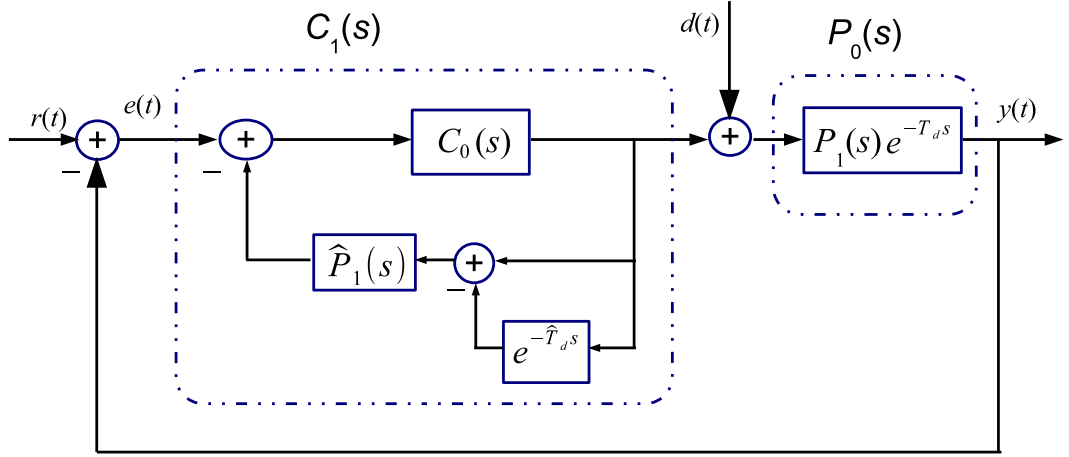


Figure 1.1: *Block diagram of a feedback system whose controller is in a Smith predictor structure*

In this figure, overall controller $C_1(s)$ is

$$C_1(s) = \frac{C_0(s)}{1 + C_0(s)\hat{P}_1(s)(1 - e^{-\hat{T}_d s})}$$

In case $\hat{P}_1(s) = P_1(s)$ and $\hat{T}_d = T_d$, the closed loop transfer function can be written as

$$\begin{aligned} T_0(s) &= \frac{C_1(s)P_1(s)e^{-T_d s}}{1 + C_1(s)P_1(s)e^{-T_d s}} \\ &= \frac{\frac{C_0(s)}{1 + C_0(s)P_1(s)(1 - e^{-T_d s})}P_1(s)e^{-T_d s}}{1 + \frac{C_0(s)}{1 + C_0(s)P_1(s)(1 - e^{-T_d s})}P_1(s)e^{-T_d s}} \\ &= \frac{C_0(s)P_1(s)}{1 + C_0(s)P_1(s)} e^{-T_d s}. \end{aligned}$$

Consequently, time delay is removed from the characteristic equation of the closed loop system and thus the controller can be designed without time delay consideration. In other words, although physically not the case, the transfer function from reference input to output can be imagined as in the Figure 1.2. By using Smith predictor structure, controller design methods for processes without delay can be directly implemented.

Over the last 50 years, many modifications to the Smith predictor structure have been proposed in order to meet certain objectives like those below:

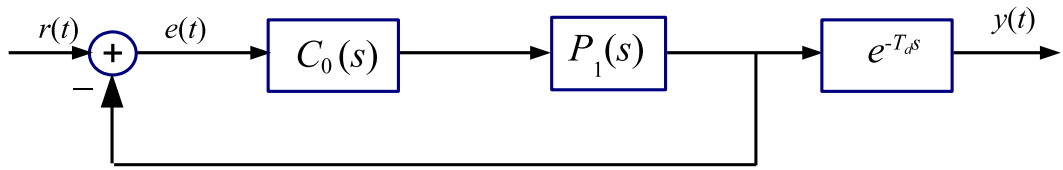


Figure 1.2: *Equivalent block diagram of Smith predictor in terms of the transfer function from input to output*

- improve setpoint response of Smith predictor based controller
- reject different kinds of disturbances
- implement this structure for various type of plants (stable, integrating, unstable)
- provide enough robustness in the presence of mismatch in the parameters and unmodeled dynamics.

Particularly, [27] proved that constant disturbance rejection cannot be achieved by using Smith predictor structure and also showed that when process delay is not the same as its nominal value, steady state error cannot be avoided in the presence of load change. Afterwards, many other modifications have been made to handle the challenge of controlling a system with integrator and transport delay, e.g., [19], modified the structure of [27] by adding a filter. Improving tracking response with two degree of freedom control structure is intended in [19]. Also, [3] introduced a new form for the control of integrator and dead time processes which dissociates the disturbance and set-point response from each other. The usage of three extra parameters supplies the capability of increasing performance. However, tuning of many parameters can cause trouble since they have no definite physical meaning. The modifications of [17]–[16], include extra feedback path from the difference of plant output and the model output to the control input. In their first work, they used a proportional controller and then the primary controller became a lead/lag controller. By using two degree of freedom controller structure, [17], provide fast disturbance suppression for constant disturbances which is caused by derivative action and fast estimation of the disturbance. Likewise, [14] offered a basic relay

auto-tuning method for the Smith Predictor and a reduced order process model in terms of a first- or second-order dynamics plus dead time was obtained .

In all afore mentioned works, the robustness issue was not explicitly analyzed. Unavoidable disturbances and uncertainty in the model parameters appear in practise. The prediction of control signals is influenced negatively by them. In fact, even if the Smith predictor is nominally stable, it is possible to destabilize the feedback system by a minor change in the process dynamics. For this purpose, a number of researches have been conducted to analyze the robustness of designed Smith predictor based controller. As an example, [11] defined multiplicative uncertainties in the model parameters to analyze the robustness in the presence of mismatch. A geometric approach is offered in [18] to define the impacts of the delay uncertainty on the stability. Also, [9] used system identification method to find out a nominal model and they determined uncertainty bound of the nominal model in the frequency domain through the uncertainty quantification method. A robust criterion for the Smith predictor was also derived in [9]. Mismatch in time delay is analyzed in [1]. Many other researchers also focused on robustness of Smith predictor, see e.g., [10] and [12].

The Smith predictor structure is used in many application areas such as telecommunication [13], [15, 5], biological systems, [25], and flexible-link robot manipulator [4]. We will design Smith predictor based controller for a flexible

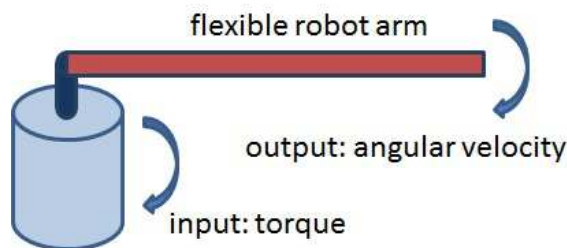


Figure 1.3: *A representation of a flexible robot arm*

robot arm, which can model a number of physical systems, with time delay which can be used for several purposes. A typical robot arm can be represented as in Figure 1.3. The motor placed at the joint applies torque that give action to robot

arm. The physical signals such as angular velocity, position and acceleration of robot arm are measured by sensors (e.g. gyroscope, resolver, encoder). In control applications, these measurements are used to compare with desired values and then convenient current is produced to generate torque. For a velocity control system for a robot arm, the procedure can be seen as in Figure 1.4. To design an effective controller, it is essential to analyze this system properly. We need to know how applied torque influences the velocity of the robot arm.

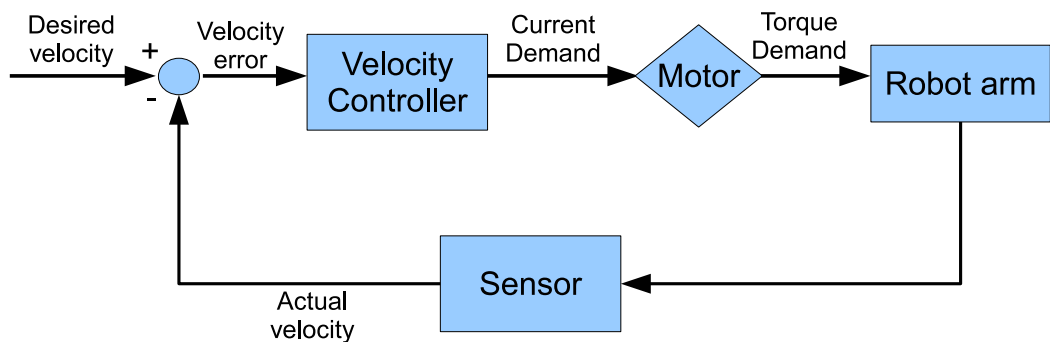


Figure 1.4: *Velocity control system for a robot arm*

Designing a controller for flexible models is a challenging process depending on damping ratio and resonance frequencies within the control bandwidth. In this work, we will also handle this problem in addition to handling of time delay. A linear model is used in controller design for simplicity. We also focus on coping with the modeling error and system uncertainties. The mismatch in the system parameters and unmodeled dynamics are also analyzed. Stability robustness of the controller obtained is also investigated.

A modified type of controller in the structure of Smith predictor will be designed for a flexible robot arm including integrator and time delay. In design, we will determine some interpolation conditions which satisfy some performance criteria and handle the previously described problem of [27] for different cases. As known, internal model principle [6] became very popular for the aim of disturbance rejection and set-point response after 1970's. Internal model principle implies that to reject impacts of disturbances and to track a reference signal,

controller should have the copies of the disturbance and reference signal generators. In our design, Smith predictor structure is integrated with internal model principle through the interpolation conditions.

Controller parametrization, [28], is used to determine the structure of $C_0(s)$ shown in Figure 1.1. This parametrization method allows widest freedom in controller parameters and this results in improved performance, both in set-point response and disturbance rejection. We also pay attention to the problem of system robustness under the impact of the aforementioned unmodeled dynamics. By taking into consideration trade-off between performance and robustness, different designs will be obtained. Advantages and drawbacks of each design are discussed with respect to both robustness and performance. Designed controllers are compared with [17] which is proved to offer good performance. Many recent application oriented papers in this area consider [17] as the baseline for comparison, [8], [26]. Our simulation results generally show that improved performance can be obtained in the presence of uncertainties.

As an alternative implementation of our controller, irrational function $e^{-T_d s}$ in Figure 1.1 is replaced with a rational function which is obtained with Pade approximation after controller design. It provides convenience in implementation of the controller for a real robot arm. It is also helpful to see the structure of overall controller, $C_1(s)$. Moreover, various filters are used to satisfy certain specifications. For instance, in order to filter the torque, which is controller output, we employ an approximate inverse of flexible modes. This filter enables to suppress high order modes generated by flexible modes of robot arm. When two-degree of freedom controller scheme is considered, another stable first-order low-pass filter is designed to cancel some of the higher dynamics of the closed loop system. With this filter, reference signal is filtered and good tracking response is achieved.

The thesis is organized as follows. In Chapter 2, structure of the plant is defined. Different controller designs are proposed to stabilize this plant. Effects of the reference filter and usage of the Pade approximation are shown. In Chapter 3, robustness and performance of designed controllers are investigated. Performance

is analyzed in terms of both set-point tracking and disturbance rejection. Stability robustness analysis is done for parametric and dynamic uncertainties. Concluding remarks are made in Chapter 4.

Table 1.1: Notation

s	Laplace variable
t	Time variable
$P(s)$	Real system between torque demand and velocity
$P_0(s)$	Nominal system
$P_1(s)$	Delay-free part of nominal system
r_p	Position demand
r_v	Velocity demand
$d(t)$	Disturbance
J	Inertia
K	Gain
\hat{K}	Estimated gain
T_d	Time delay
\hat{T}_d	Estimated time delay
$R_0(s)$	Flexible modes
$\hat{R}_0(s)$	Estimated flexible modes
$\hat{R}_\epsilon^{-1}(s)$	Approximate inverse of flexible modes
$\Delta_m(s)$	Multiplicative uncertainty
$H(s)$	First order reference filter
ω_h	Cut-off frequency of reference filter
$G_0(s)$	Open loop transfer function
$T_0(s)$	Closed loop transfer function for velocity control system
$P_{p1}(s)$	Delay-free part of closed loop transfer function of $T(s)$
$T_p(s)$	Closed loop transfer function for position control system
$T_{yd}(s)$	Transfer function between disturbance and output
$C_v(s)$	Smith predictor based velocity controller
$C_{0v}(s)$	Internal controller in velocity control
$C_p(s)$	Smith predictor based position controller
$C_{0p}(s)$	Internal controller in position control

Chapter 2

SMITH PREDICTOR BASED CONTROL OF THE ROBOT ARM

2.1 Preliminaries

Definition 2.1.1. *A transfer function $H(\cdot) \in \mathbb{R}H_\infty$ if it is analytic in \mathbb{C}_+ and following condition is satisfied*

$$\|H\|_\infty = \sup_{\operatorname{Re}(s) > 0} |H(s)| < \infty \quad (2.1)$$

Let $P_c(s)$ be a linear transfer function of a plant. In order to find all controllers C stabilizing $P_c(s)$ in the feedback system shown in Figure 2.1, following algorithm is proposed by [28]:

- [i] Nominal plant $P_c(s)$ is written in terms of coprime rational and stable transfer functions, $N_p(s)$, $D_p(s)$, i.e $N_p, D_p \in \mathbb{R}H_\infty$

$$P_c(s) = \frac{N_p(s)}{D_p(s)}$$

[ii] Two other stable $X(s)$ and $Y(s)$ transfer functions which satisfy the following Bezout equation are obtained:

$$XN_p + YD_p = 1$$

Theorem 2.1.1 (Controller Parametrization). *The set of all all controllers which guarantee the internal stability of the feedback system in Figure 2.1 is given by*

$$C(s) = \frac{X + D_p Q}{Y - N_p Q} : \quad Q \in \mathbb{R}H_\infty, \quad Q \neq YN_p^{-1}$$

Let us choose $P_c(s) = \frac{1}{s-1}$.

[i] In order to get stable $N_p(s)$ and $D_p(s)$, we can determine

$$N_p(s) = \frac{1}{s+a} \quad \text{and} \quad D_p(s) = \frac{s-1}{s+a} \quad \text{where } a > 0$$

[ii] From Bezout equation,

$$Y(s) = \frac{1 - N_p(s)X(s)}{D_p(s)}$$

Since $D_p(1) = 0$, we need to choose $1 - N_p(1)X(1) = 0$ to get stable $Y(s)$. It results in $X(1) = a + 1$. By choosing $X(s) = a + 1$ which is stable, we obtain $Y(s) = 1$.

According to the Theorem 2.1.1, corresponding $C(s)$ which stabilizes $P_c(s)$ can be found as

$$C(s) = \frac{a+1 + \frac{s-1}{s+a}Q(s)}{1 - \frac{1}{s+a}Q(s)} : \quad Q \in \mathbb{R}H_\infty$$

Theorem 2.1.2 (L'Hôpital Rule). *Suppose f and g are differentiable functions of x on (a, b) and*

$$\lim_{s \rightarrow a^+} f(x) = \lim_{s \rightarrow a^+} g(x) = 0$$

and the limit

$$\lim_{s \rightarrow a^+} \frac{f'(x)}{g'(x)} = M$$

exists, then the limit

$$\lim_{s \rightarrow a^+} \frac{f(x)}{g(x)} = M$$

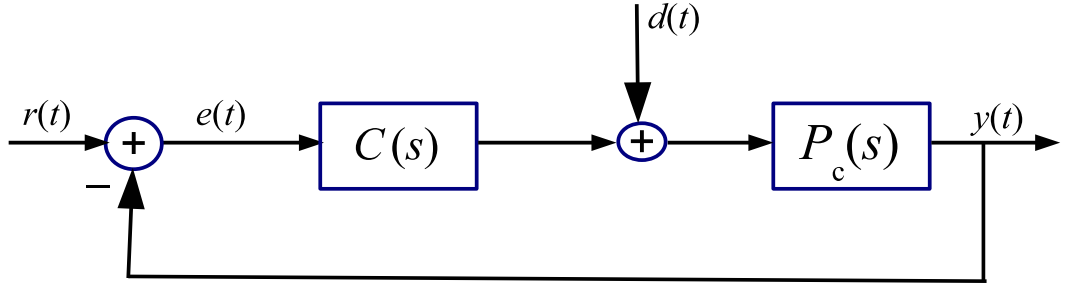


Figure 2.1: *Closed-loop feedback system*

2.2 Plant Structure

There are many different types of two degree-of freedom robot manipulators used in industry and academic works. In this thesis, we will focus on a particular type of robot arm which is depicted in Figure 1.3. Control input is the torque applied by the motor and the angular velocity is taken to be the output. We already know from physical laws that the transfer function from torque to velocity includes an integrator which appears due to Newton's law. Also, there will be a gain factor which is inversely proportional to inertia. The exact value of the gain depends on material geometry, mechanical signal amplifiers and scaling factors in actuator. Time delay comes into the system as a result of the distance between sensor and actuator, sampling and slack between the mechanical components. In addition to that, right-half plane zeros emerge as the result of different location of actuator and sensor. Phase shift caused by this situation can be modeled as time delay. Lastly, we expect some vibrations on the robot arm at high frequencies as a consequence of slack in the gear and material structure.

There are many approaches to modeling and system identification for flexible robot arm, see e.g. [7], [23] and their references. We will assume that nominal parameters for the flexible modes are obtained from parameter estimation, and any non-minimum phase part is absorbed into the time delay. Hence the plant transfer function from torque to angular velocity is in the form

$$P(s) = \frac{K}{s} e^{-T_d s} R_0(s) \quad (2.2)$$

where $K > 0$ is the gain, $T_d > 0$ is the time delay and $R_0(s)$ is the minimum phase transfer function in the form

$$R_0(s) = \frac{\omega_0^2}{s^2 + 2\zeta_0\omega_0s + \omega_0^2} \prod_{k=1}^n \frac{(s^2/\tilde{\omega}_k^2) + 2\tilde{\zeta}_k(s/\tilde{\omega}_k) + 1}{(s^2/\omega_k^2) + 2\zeta_k(s/\omega_k) + 1}$$

where $0 < \omega_0 < \tilde{\omega}_k < \omega_k$ are the resonant and anti-resonant frequencies, and $\tilde{\zeta}$, ζ , are the damping factors, taking values between 0 and 1. It is assumed that the above parameters are estimated from system identification, but when it comes to stability robustness analysis, uncertainty in $R_0(s)$ will be considered. Note that $R_0(j\omega) \approx 1$ for all $0 \leq \omega \ll \omega_0$.

2.3 Smith Predictor Based Controller Design for Velocity Control

In this section, Smith predictor based controller will be designed for the plant in (2.2). Designed controller is supposed to satisfy following three objectives:

- robust stability
- tracking reference signal
- disturbance attenuation

The structure of proposed Smith predictor based controller for this model is shown in Fig. 2.2. As seen from Fig. 2.2, the controller C_v is

$$C_v(s) = \frac{\hat{R}_\varepsilon(s)^{-1}}{\hat{K}} \left(\frac{C_{0v}(s)}{1 + C_{0v}(s) \frac{1 - e^{-\hat{T}_d s}}{s}} \right) \quad (2.3)$$

Here, $\hat{R}_\varepsilon^{-1}(s) = \hat{R}_0^{-1}(s)/(1 + \varepsilon s)^2$ is the approximate inverse of the term due to flexible modes, with $0 < \varepsilon \ll \omega_n^{-1}$; \hat{R}_0^{-1} is in the same form of $R_0(s)$ except that its parameters are the estimated values of ω_i , ζ_i , $\tilde{\omega}_i$, $\tilde{\zeta}_i$ for $i = 0, 1, \dots, n$, which are not necessarily matching the exact values used in $R_0(s)$. The free part of the controller

is $C_{0v}(s)$ and it is to be designed from the non-delayed part of the plant as in the usual Smith predictor based design. Typically, $H(s) = 1$ and does not play a role in the feedback system stability analysis, nor in the disturbance attenuation problem. When two-degree of freedom controller scheme is considered, the stable filter $H(s)$ is designed to improve the tracking performance (see Section 2.5).

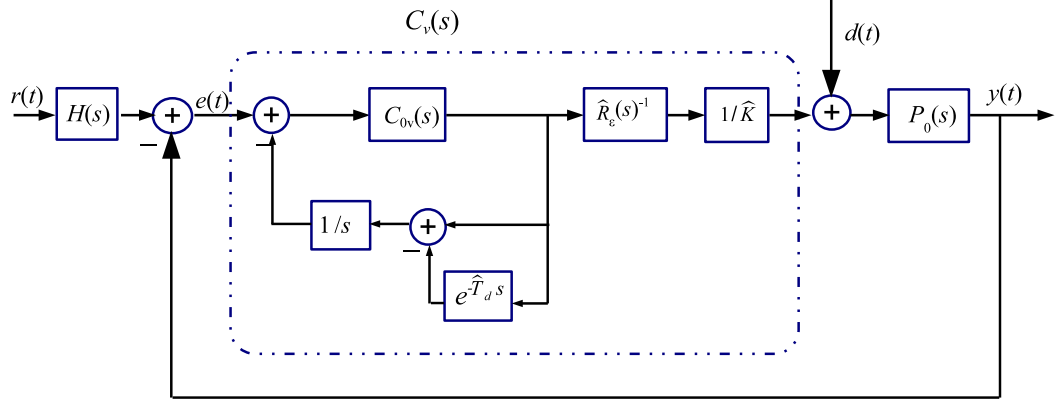


Figure 2.2: *Proposed Smith Predictor Based Controller Structure*

Keeping in mind the above conditions, stability of the feedback system must be guaranteed. With the controller structure $C_v(s)$, when the plant is known $P(s) = P_0(s)$, the characteristic equation of closed-loop system is

$$1 + C_{0v}(s)\frac{1}{s} = 0 \quad (2.4)$$

which means that $C_{0v}(s)$ must be designed to stabilize the integrator. If $P_c(s) = \frac{1}{s}$, then the set of all controllers which stabilizes P_c are found from Theorem 2.1.1. To find this set, let $P_c(s) = \frac{N_p(s)}{D_p(s)}$, where $D_p(s) = \frac{s}{s+a}$ and $N_p(s) = \frac{1}{s+a}$ with $a > 0$ is a parameter to be chosen via pole placement method as shown below.

From Theorem 2.1.1, all stabilizing controllers for $P_1(s)$ are parameterized as:

$$C_{0v}(s) = \frac{X(s) + D_p(s)Q(s)}{Y(s) - N_p(s)Q(s)} \quad (2.5)$$

where $Q \in H_\infty$ and $Q \neq YN_p^{-1}$. Here $X, Y \in H_\infty$ are functions satisfying

$$N_p(s)X(s) + D_p(s)Y(s) = 1 \quad (2.6)$$

It is clear from (2.6) that

$$Y(s) = \frac{1 - N_p(s)X(s)}{D_p(s)} \quad (2.7)$$

Since $D_p(0) = 0$, $X(0)$ must be equal to $\frac{1}{N_p(0)}$. It means $X(0) = a$. Since $X(s)$ should be stable, simply it can be chosen as $X(s) = a$. Then, from (2.7), $Y(s)$ can be found as:

$$Y(s) = \frac{1 - \frac{1}{s+a}a}{\frac{s}{s+a}} = \frac{(s+a) - a}{s} = 1$$

If all functions are put into (2.5), internal controller is

$$C_{0v}(s) = \frac{a + \frac{s}{s+a}Q(s)}{1 - \frac{1}{s+a}Q(s)} = \frac{as + a^2 + sQ(s)}{s + a - Q(s)}. \quad (2.8)$$

Now, the problem reduces to designing a $Q(s)$ depending on different requirements of performance and robustness. It must be chosen as a proper function and degree of $Q(s)$ changes according to the interpolation conditions. Minimum degree of $Q(s)$ satisfying interpolation condition requirement is given by

$$\text{Minimum degree of } Q(s) = \text{Number of interpolations} - 1 \quad (2.9)$$

We will obtain four different designs to satisfy different objectives.

2.3.1 Smith Predictor Based Controller for Constant Disturbance Rejection

In this design, the objectives are suppressing constant disturbances and tracking unit reference signal without steady-state error. Obtained controller will be in the structure of a PI controller. For this aim, the overall controller, $C_v(s)$, is required to be Type-1 controller having a pole at $s = 0$. This condition is translated into

$$\lim_{s \rightarrow 0} C_v(s) = \infty \implies \lim_{s \rightarrow 0} \left(1 + C_{0v}(s) \frac{(1 - e^{-\hat{T}_d s})}{s} \right) = 0$$

Since there is an indeterminate form of $\frac{0}{0}$, L'Hôpital Rule is used to obtain an interpolation condition on $C_{0v}(s)$. From Theorem 2.1.2, we obtain $1 + T_d C_{0v}(0) =$

0 which means

$$C_{0v}(0) = -\frac{1}{T_d}. \quad (2.10)$$

By using (2.8), the structure of $C_{0v}(s)$ is found as

$$C_{0v}(0) = \frac{a^2}{a - Q(0)},$$

and for $Q(s)$, the interpolation condition turns into

$$Q(0) = a(1 + a\hat{T}_d).$$

Since only one interpolation condition is stated on $C_{0v}(s)$, $Q(s)$ is chosen as constant for minimum-degree $C_{0v}(s)$ from (2.9). By using $Q(s) = a(1 + a\hat{T}_d)$, corresponding $C_{0v}(s)$ is obtained as

$$C_{0v}(s) = \frac{(2a + a^2\hat{T}_d)s + a^2}{s - a^2\hat{T}_d}.$$

With the above design, when $P = P_0$, $\hat{K} = K$, $\hat{T}_d = T_d$, $\hat{R}_0 = R_0$ and $\varepsilon \rightarrow 0$, the closed-loop transfer function from r to y in Fig. 2.2, is $T_{ry}(s) = T_0(s)H(s)$, where $T_0 = P_0C_v(1 + P_0C_v)^{-1}$, and it reduces to

$$T_0(s) = \frac{(2a + a^2\hat{T}_d)s + a^2}{(s + a)^2} e^{-T_d s}, \quad (2.11)$$

where $a > 0$ is chosen to place the closed loop system poles at the desired location. It is also obvious to see that closed loop system zeros are the same as the zeros of $C_{0v}(s)$ in this design.

2.3.2 Smith Predictor Based Controller Rejecting Constant and Ramp Disturbances

In this section, the design objective is suppressing constant and ramp disturbances in steady-state. To satisfy this condition, $C_v(s)$ is entailed to have two poles at $s = 0$. This condition is translated to

$$\lim_{s \rightarrow 0} sC_v(s) = \infty \implies \lim_{s \rightarrow 0} \frac{s + C_{0v}(s)(1 - e^{-\hat{T}_d s})}{s^2} = 0 \quad (2.12)$$

where indeterminate form of 0/0 is detected. To handle with this problem, L'Hôpital Rule is applied on (2.12). Corresponding limit condition is

$$\lim_{s \rightarrow 0} \frac{1 + C_{0v}(s)\widehat{T}_d e^{-\widehat{T}_d s} + C'_{0v}(s)(1 - e^{-\widehat{T}_d s})}{2s} = 0 \quad (2.13)$$

The nominator of the equation in (2.13) must be equal to 0 at $s = 0$ to cancel the pole at $s = 0$. First design criterion is obtained as

$$C_{0v}(0) = -\frac{1}{\widehat{T}_d}. \quad (2.14)$$

which is consistent with the interpolation condition obtained in (2.10). At this point, indeterminate form of 0/0 emerges again. By performing L'Hôpital Rule once more, (2.13) turns into

$$\lim_{s \rightarrow 0} \frac{-C_{0v}(s)\widehat{T}_d^2 e^{-\widehat{T}_d s} + C'_{0v}(s)\widehat{T}_d e^{-\widehat{T}_d s} + C''_{0v}(s)(1 - e^{-\widehat{T}_d s}) + C'_{0v}(s)\widehat{T}_d e^{-\widehat{T}_d s}}{2} = 0$$

When the value of $C_{0v}(0)$ found in (2.14) is inserted, the second design criterion is acquired as

$$C'_{0v}(0) = -\frac{1}{2}. \quad (2.15)$$

The design criteria (2.14)-(2.15) are converted into the interpolation conditions on $Q(s)$ by using (2.8):

$$Q(0) = a(1 + a\widehat{T}_d) \quad (2.16)$$

$$Q'(0) = 1 - \frac{(a - Q(0))(1.5a + 0.5Q(0))}{a^2} \quad (2.17)$$

The problem now is to find such a $Q(s)$ that (2.16) and (2.17) are satisfied. Since there are two interpolation conditions, it is clear from (2.9) that for minimum-degred $Q(s)$ the structure of $Q(s)$ must be as below:

$$Q(s) = \frac{(bs + c)}{(s + e)}. \quad (2.18)$$

Here e is a free parameter. Like the parameter a , it also determines the location of closed loop poles. The other parameters b, c are calculated depending on the interpolation conditions. Their values are:

$$c = Q(0)e$$

and

$$b = Q'(0)e + \frac{c}{e}.$$

When $Q(s)$ is inserted into (2.8), the structure of $C_0(s)$ obtained is shown below:

$$C_{0v}(s) = \frac{(a+b)s^2 + (al_1+c)s + al_2}{s^2 + (l_1-b)s + (l_2-c)} \quad (2.19)$$

where $l_1 = a + e$ and $l_2 = ae$. With the above design and the assumption of $P = P_0$, $\hat{K} = K$, $\hat{T}_d = T_d$, $\hat{R}_0 = R_0$ and $\varepsilon \rightarrow 0$, the closed loop transfer function is

$$T_0(s) = \frac{(a+b)s^2 + (al_1+c)s + al_2}{(s+a)^2(s+e)} e^{-T_d s} \quad (2.20)$$

2.3.3 Smith Predictor Design To Reject Constant and Sinusoidal Disturbance

In this section, for the plant given in (2.2), the controller $C_v(s)$ is required to satisfy these two conditions:

1. $C_v(s)$ must be Type 1, to suppress constant disturbance in steady state.
2. periodic disturbances $d(t)$ with known frequency, ω_d , must be rejected in steady state.

The interpolation condition to satisfy the first condition has already been evaluated in Section 2.3.1, which gave (2.16) as the first design criterion. According to internal model principle, [6], to satisfy the second condition, $C_v(s)$ must have poles at $s = \pm j\omega_d$:

$$\lim_{s \rightarrow j\omega_d} C_v(s) = \infty \implies \lim_{s \rightarrow j\omega_d} \left(1 + C_{0v}(s) \frac{(1 - e^{-\hat{T}_d s})}{s} \right) = 0$$

which means

$$C_{0v}(j\omega_d) = \frac{-j\omega_d}{1 - e^{-j\hat{T}_d \omega_d}}. \quad (2.21)$$

By using 2.8, the value of $C_{0v}(j\omega_d)$ is also found as

$$C_{0v}(j\omega_d) = \frac{aj\omega_d + a^2 + j\omega_d Q(j\omega_d)}{j\omega_d + a - Q(j\omega_d)}. \quad (2.22)$$

When (2.21) and (2.22) are employed, this gives us the second interpolation condition on $Q(s)$:

$$Q(j\omega_d) = \frac{(j\omega_d + a - ae^{-j\omega_d\hat{T}_d})(j\omega_d + a)}{(j\omega_d)e^{-j\omega_d\hat{T}_d}}. \quad (2.23)$$

Thus two interpolation conditions are obtained on $Q(s)$. Since $Q(s)$ is a rational function, only one interpolation condition is sufficient to incorporate complex roots. However, we will consider the case for $Q(-j\omega_d)$ in deciding the minimum degree structure of $Q(s)$. We postulate the following minimum degree $Q(s)$:

$$Q(s) = \frac{bs^2 + cs + d}{s^2 + es + f}.$$

Here $e, f > 0$ are free parameters; once these free parameters are chosen, b, c and d are determined from the interpolation conditions (2.16) and (2.23). Their values are

$$b = \frac{\operatorname{Re} \left(\frac{j\omega_d + a - ae^{-j\omega_d\hat{T}_d}(j\omega_d + a)}{j\omega_d e^{-j\omega_d\hat{T}_d}} (f + j\omega_d e - \omega_d^2) \right) - d}{-\omega_d^2},$$

$$c = \frac{\operatorname{Im} \left(\frac{j\omega_d + a - ae^{-j\omega_d\hat{T}_d}(j\omega_d + a)}{j\omega_d e^{-j\omega_d\hat{T}_d}} (f + j\omega_d e - \omega_d^2) \right)}{\omega_d},$$

$$d = fa(1 + a\hat{T}_d).$$

In conclusion, $C_{0v}(s)$ turns into

$$C_{0v}(s) = \frac{(a+b)s^3 + (l_1a+c)s^2 + (l_2a+d)s + al_3}{s^3 + (l_1-b)s^2 + (l_2-c)s + (l_3-d)}, \quad (2.24)$$

where $l_1 = e + a$, $l_2 = f + ae$, $l_3 = af$.

With the above design, when $P = P_0$, $\hat{K} = K$, $\hat{T}_d = T_d$, $\hat{R}_0 = R_0$ and $\varepsilon \rightarrow 0$, the closed-loop transfer function from r to y in Fig. 2.2, is $T_{ry}(s) = T_0(s)H(s)$ where $T_0 = P_0C_v(1 + P_0C_v)^{-1}$, and it reduces to

$$T_0(s) = \frac{N_T(s)}{(s^2 + es + f)(s + a)^2} e^{-T_d s},$$

$$N_T(s) = a(s + a)(s^2 + es + f) + s(bs^2 + cs + d),$$

where $a > 0$, $e > 0$ and $f > 0$ are chosen to place the closed loop system poles at the desired locations

2.3.4 Smith Predictor Design To Reject Constant, Ramp and Sinusoidal Disturbance

In this section, $C_v(s)$ is restricted to be Type 2 as different from the design in Section 2.3.3. All interpolation conditions found in the previous sections

$$Q(0) = a(1 + a\hat{T}_d), \quad (2.25)$$

$$Q'(0) = 1 - \frac{(a - Q(0))(1.5a + 0.5Q(0))}{a^2}, \quad (2.26)$$

$$Q(j\omega_d) = \frac{(j\omega_d + a - ae^{-j\omega_d\hat{T}_d})(j\omega_d + a)}{(j\omega_d)e^{-j\omega_d\hat{T}_d}} \quad (2.27)$$

are necessary to be satisfied for this purpose. Postulated minimum-degree $Q(s)$ which accomplishes these interpolation conditions is

$$Q(s) = \frac{(bs^2 + cs + d)(s + m)}{(s^2 + es + f)(s + n)}$$

Here e, f, n are free parameters. The values of other parameters b, c, d, m are determined depending on these free parameters and (2.25)-(2.26)-(2.27). When we choose $K_1 = nfQ(0)$:

$$md = K_1$$

can be easily written from (2.25). Also for $K_2 = Q'(0)nf + Q(0)(f + en)$,

$$mc + d = K_2$$

is obtained from (2.26). Lastly for

$$K_3 = \text{Re}(Q(j\omega_d))(-\omega_d + f\omega_d + en\omega_d) + \text{Im}(Q(j\omega_d))(-n\omega_d^2 - \omega_d^2e)$$

$$K_4 = \text{Re}(Q(j\omega_d))(-n\omega_d^2 - \omega_d^2e) - \text{Im}(Q(j\omega_d))(-\omega_d + f\omega_d + en\omega_d)$$

we can get

$$-b\omega_d^3 + K_2\omega_d = K_3 \quad (2.28)$$

$$-mb\omega_d^2 + K_1 - c\omega_d = K_4 \quad (2.29)$$

depending on (2.27) By using all these equations,

$$b = \frac{K_3 - K_2\omega_d}{-\omega_d^3}$$

To evaluate the values of the other parameters c, d , we need to solve the equation

$$bm^3 + \left(\frac{K_4 - K_1}{\omega_d^2} \right) m^2 + K_2 m - K_1 = 0. \quad (2.30)$$

The real root of this equation is chosen as the value of m . After that, the other values are obtained like below:

$$d = \frac{K_1}{m}$$

and

$$c = \frac{K_2 - d}{m}$$

All parameters are inserted into (2.19) to obtain corresponding controller. We find $C_0(s)$ as

$$C_{0v}(s) = \frac{(a+b)s^4 + (l_1a + l_5)s^3 + (l_2a + l_6)s^2 + (l_3a + l_7)s + l_4a}{s^4 + (l_1 - b)s^3 + (l_2 - l_5)s^2 + (l_3 - l_6)s + (l_4 - l_7)} \quad (2.31)$$

$l_1 = a(n + e + 1)$, $l_2 = (f + en) + a(n + e)$, $l_3 = fn + a(f + en)$, $l_4 = afn$, $l_5 = bm + c$, $l_6 = cm + d$ and $l_7 = md$. The transfer function from reference input to output is

$$T_0(s) = \frac{N_T(s)}{(s^2 + es + f)(s + n)(s + a)^2} e^{-T_d s} \quad (2.32)$$

$$N_T(s) = a(s + a)(s^2 + es + f)(s + n) + s(bs^2 + cs + d)(s + m) \quad (2.33)$$

2.4 Pade Approximation of Time Delay for Controller Implementation

In this section, the controller structure proposed in 2.3 is reorganized by using Pade approximation which is commonly used in control applications to replace irrational time delay term with a stable rational transfer function. We will use Pade approximation for

$$C_{v1}(s) = \frac{1}{\widehat{K}} \left(\frac{C_{0v}(s)}{1 + C_{0v}(s) \frac{1 - e^{-\widehat{T}_d s}}{s}} \right) \quad (2.34)$$

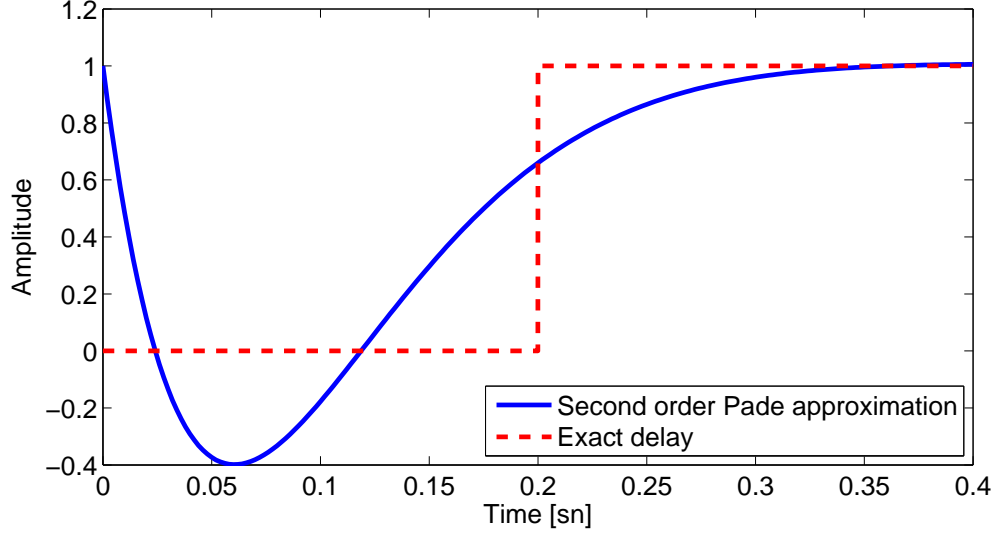


Figure 2.3: *Step response comparison for $T_d = 0.2$*

which is a factor of $C_v(s)$. The irrational function $e^{-T_d s}$ can be approximated by a rational function via

$$e^{-T_d s} \cong \frac{1 - k_1 s + k_2 s^2 + \dots \pm k_n s^n}{1 + k_1 s + k_2 s^2 + \dots + k_n s^n},$$

where n is the order of the approximation. When n gets larger, the approximation gets close to the exact value. On the other hand, some numerical problems emerge to compute the polynomial coefficients, [20]. In this work, using second order Pade approximation of time delay suffices to acquire a satisfactory result:

$$e^{-T_d s} \cong \frac{1 - \frac{T_d}{2}s + \frac{T_d^2}{12}s^2}{1 + \frac{T_d}{2}s + \frac{T_d^2}{12}s^2}$$

Utilizing a rational transfer function not only facilitates the implementation of the controller in practical applications, but also prevents controller from having infinitely many poles. We can also see the structure of the controller clearly with this approximation. If time-delay is small, corresponding controllers for different designs proposed in Section 2.3 are shown in Table 2.1. It should be noted that static gains of the original controller and approximated controller are compensated via K_{1p} . Coefficients of the controller are determined by the closed loop

Table 2.1: Obtained controllers via second order Pade approximation of the delay

Designs	Obtained C_{v1} structure
Design in Section 2.3.1	$K_{1p} \left(\frac{s + h_1}{s} \right)$
Design in Section 2.3.2	$K_{1p} \left(\frac{s^2 + h_1s + h_2}{s^2} \right)$
Design in Section 2.3.3	$K_{1p} \left(\frac{s + h_1}{s} \right) \left(\frac{s^2 + h_2s + h_3}{s^2 + \omega_d^2} \right)$
Design in Section 2.3.4	$K_{1p} \left(\frac{s^2 + h_1s + h_2}{s^2} \right) \left(\frac{s^2 + h_3s + h_4}{s^2 + \omega_d^2} \right)$

system poles location as explained in Section 2.3. Obtained controller structures completely satisfy the design requirements and the overall controllers include the poles at desired locations. By using this approach, it is also possible to enlarge the controller structures for other purposes. By using internal model principle, we can get the poles at any desired points for the controller. Since controller parametrization guarantees internal stability of the system, we do not need to do any other regulation or calculation on the parameters after approximation.

2.5 The Effects of Reference Filter

The aim of the filter $H(s)$ in Figure 2.4 is to develop tracking response by suppressing the high order dynamics of the feedback system. It should be noted that existence of the reference filter has no effect on the transfer function from disturbance to output. Basically, we choose a stable and strictly proper first order $H(s)$ with $H(0) = 1$. One particular choice is

$$H(s) = \frac{1}{1 + s/\omega_h}$$

where cut-off frequency, ω_h , is the free design parameter. Typically, cut-off frequency is chosen to cancel the fastest negative real axis zero of $T_0(s)$. Since the zeros of $T_0(s)$ and $C_{0v}(s)$ are the same, $C_{0v}(s)$ is taken into consideration for

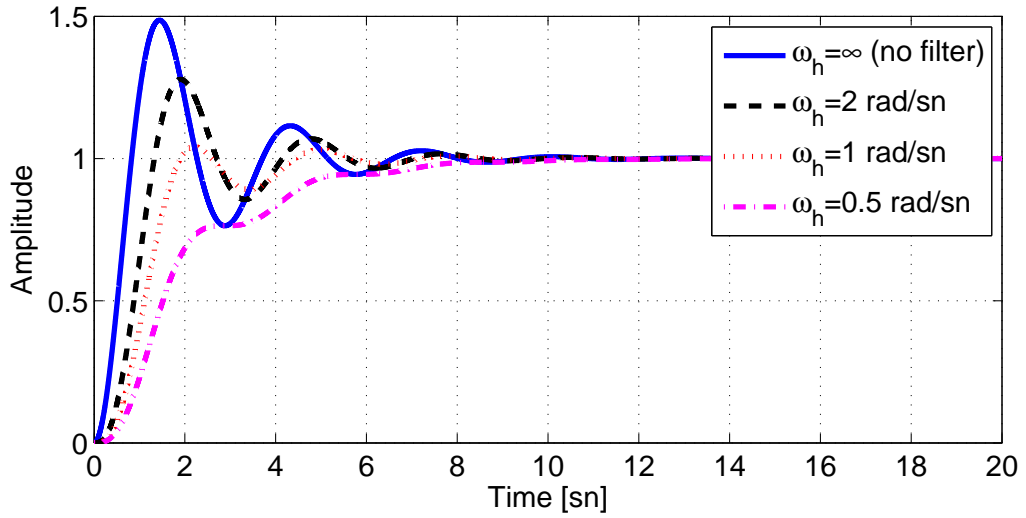


Figure 2.4: *Unit step response of a closed loop system for different cut-off frequencies*

this purpose. The value of the cut-off frequency is also dependent on the design requirements. When the filter does not exist in the system, we can say $\omega_h = \infty$ for this situation. If cut-off frequency of the system is reduced, overshoot of the output signal decreases. Also there is such a cut-off frequency after which the overall system behaves like an overdamped system. On the other hand, diminution of the cut-off frequency affects the rising time negatively. The response of the system slows down. Hence, cut-off frequency of the filter is chosen according to the design requirements on overshoot and rise time of the system. For illustrative purpose, we choose a plant $P_c(s) = \frac{1}{s(s+1)}$ and a proportional stabilizing controller $C(s) = 5$. Unit step response of this closed loop system can be seen in Figure 2.4 for different cut-off frequencies of the filter. It is clear from this figure that overshoot of the output is maximum when there is no reference filter in the system and there is no overshoot observed for $\omega_h = 0.5$ rad/sn. On the other hand, the fastest response of the system is obtained in the absence of reference filter.

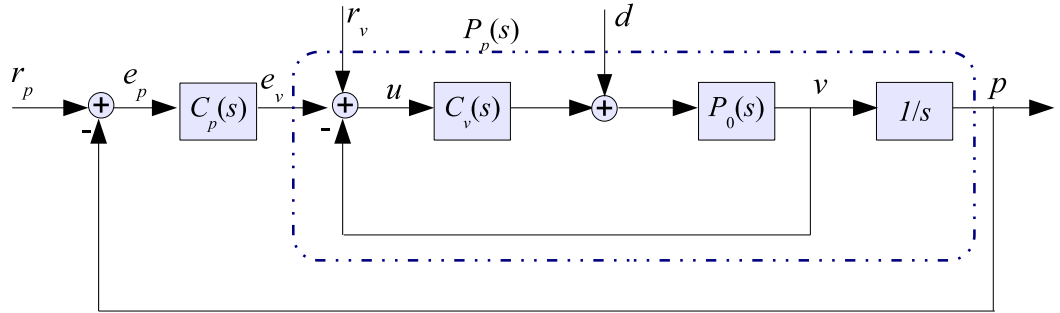


Figure 2.5: Hierarchical control structure for position control

2.6 Smith Predictor Design For Position Control

Hierarchical control structure is used to control the position of the robot arm. To obtain such a structure, a controller is designed for the plant in inner loop. By taking this controller into consideration, second controller is designed as in Figure 2.5. Since position is the integral of velocity, the transfer function from applied torque to position is $P_0(s)/s$. However, we do not design a controller directly for this plant to control position. Position controller generates velocity demand and then this demand determines how much torque will be produced. We have already designed 4 different types of $C_v(s)$ in previous section for velocity loop. Among these designs, we will just use the design in Section 2.3.1 when the position controller is employed. The position controller is designed to stabilize $T_0(s)/s$, where $T_0(s)$ is closed loop transfer function of velocity control system as indicated in (2.11). We aim to place the robot arm in the desired angular position and keep the velocity value at 0° rad/sn . Hence we determine the reference signals as $r_p = 1/s$ and $r_v = 0$. We have already designed a controller for the purpose of velocity control in Section 2.3.2. By using also this controller, we will obtain a controller structure for position loop. As mentioned before, the closed loop transfer function of velocity control system is considered as plant transfer function. The fact that position is the integral of velocity is used in this transfer

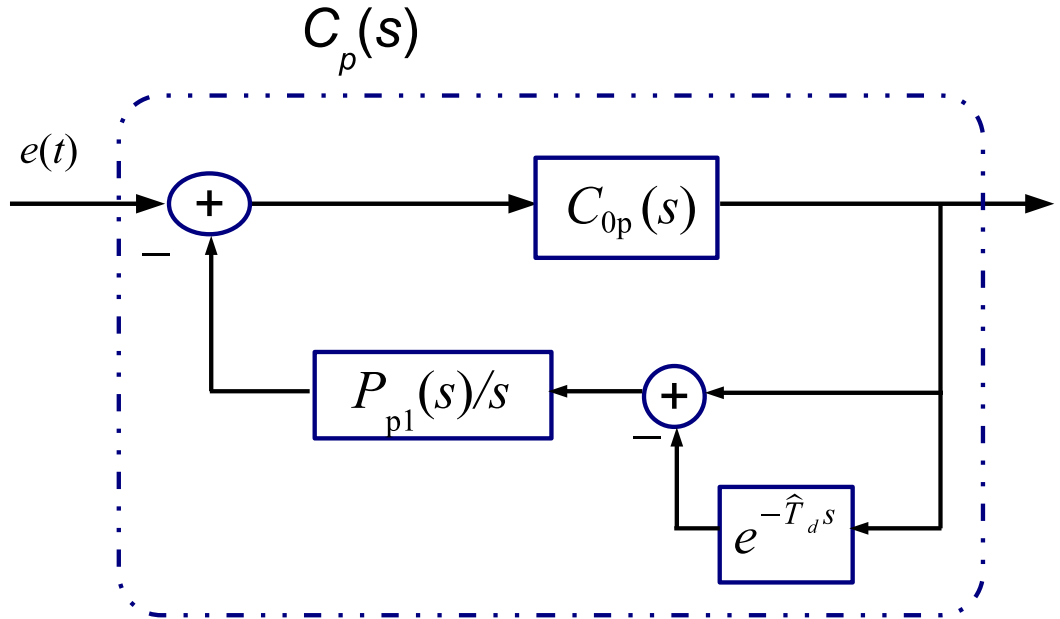


Figure 2.6: *Direct approach for position control*

function. By using (2.11), we obtain

$$P_p(s) = \frac{(2a + a^2\hat{T}_d)s + a^2}{s(s + a)^2} e^{-T_d s} \quad (2.35)$$

as the transfer function from velocity demand to position. Smith predictor based controller is used again to control position of the robot arm.

Two different methods are used to design a controller for position loop. Firstly, we will design controllers and then check in Chapter 3 whether they satisfy the requirements given above.

2.6.1 Direct Approach To Plant

In this design, internal controller, $C_{0p}(s)$, is designed for all of delay-free part of the plant given in (2.35). As seen in Figure 2.6, proposed structure of the controller is given by

$$C_p(s) = \frac{C_{0p}(s)}{1 + C_{0p}(s) \frac{P_{pl}}{s} (1 - e^{-\hat{T}_d s})}$$

where P_{p1} is delay-free part of the closed loop transfer function of velocity control system:

$$P_{p1} = \frac{(2a + a^2\widehat{T}_d)s + a^2}{(s + a)^2} \quad (2.36)$$

With the controller structure $C_p(s)$, characteristic equation of the closed loop control system is

$$1 + C_{0p}(s)\frac{P_{p1}(s)}{s} = 0$$

To guarantee the stability of feedback system, $C_{0p}(s)$ must stabilize the $\frac{P_{p1}}{s}$. The set of all stabilizing controllers are found again by using controller parametrization. To find this set, we will choose $N_p(s) = \frac{(2a + a^2T_d)s + a^2}{(s + a)^2 (s + p)}$ and $D_p(s) = \frac{s}{s + p}$ where $p > 0$ is a free parameter chosen via pole placement method. By using Theorem 2.1.1 again, all stabilizing controllers for $\frac{P_{p1}(s)}{s}$ are parameterized as:

$$C_{0p}(s) = \frac{X(s) + D_p(s)Q(s)}{Y(s) - N_p(s)Q(s)} \quad (2.37)$$

It is obvious from (2.6) again that

$$Y(s) = \frac{1 - N_p(s)X(s)}{D_p(s)} \quad (2.38)$$

To cope with the zero of $D_p(s)$ at $s = 0$, the value of $1 - N_p(s)X(s)$ must be zero at $s = 0$. As a result, we obtain $X(0) = p$. Since $X(s)$ should be stable, simply it can be chosen as $X(s) = p$. Then, from (2.38), Y can be found as:

$$Y(s) = \frac{1 - \frac{(2a+a^2T_d)s+a^2}{(s+a)^2(s+p)}p}{\frac{s}{s+p}} = \frac{s^2 + s(p + 2a) + (a^2 - a^2T_dp)}{(s + a)^2}$$

If all functions are put into (2.5),

$$\begin{aligned} C_{0p}(s) &= \frac{p + \frac{s}{s+p}Q(s)}{\frac{s^2+s(p+2a)+(a^2-a^2T_dp)}{(s+a)^2} - \frac{(2a+a^2T_d)s+a^2}{(s+a)^2(s+p)}Q(s)} \\ &= \frac{(p(s+p) + sQ(s))(s+a)^2}{(s+p)(s^2 + s(p+2a) + a^2 - a^2T_dp) - ((2a + a^2T_d)s + a^2)Q(s)}. \end{aligned} \quad (2.39)$$

Here $Q(s)$ stable transfer function is designed depending on design requirement. In this design, we want overall controller, $C_p(s)$, to have a pole at $s = 0$ which

means

$$\lim_{s \rightarrow 0} C_p(s) = \infty \implies \lim_{s \rightarrow 0} \left(1 + C_{0p}(s) \frac{(1 - e^{-\hat{T}_d s}) P_{p1}(s)}{s} \right) = 0.$$

Resulting from the indeterminate form of $0/0$, L'Hôpital Rule is employed to acquire the interpolation condition on $C_0(s)$. Obtained condition is as the same the one in the velocity controller:

$$C_{0p}(0) = -\frac{1}{T_d}. \quad (2.40)$$

When this outcome is placed in (2.39), we attain

$$\frac{p^2 a^2}{p(a^2 - a^2 T_d p) - a^2 Q(0)} = -\frac{1}{T_d}$$

which implies $Q(0) = p$. We simply choose $Q(s) = p$ and consequently we get C_{0p} as

$$C_{0p} = \frac{(s + a)^2 (2ps + p^2)}{s^3 + s^2(2a + 2p) + s(p^2 + a^2 - 2a^2 T_d p) - a^2 T_d p^2}$$

As the consequence, the closed loop transfer function is

$$T_p = \frac{(2ps + p^2) ((2a + a^2 T_d)s + a^2)}{(s + a)^2 (s + p)^2} e^{-T_d s}.$$

2.6.2 Indirect Approach To Plant

In this design, we will use $P_{p1}(s)$ and $\frac{1}{s}$ separately inside the controller. While $P_{p1}(s)$ is multiplied with time delay term as seen in Figure 2.7, the integrator term is used as in the velocity control loop. Proposed controller structure is

$$C_p(s) = \frac{C_{0p}(s)}{1 + C_{0p}(s) \frac{(1 - P_{p1} e^{-\hat{T}_d s})}{s}}.$$

The closed loop transfer function is

$$\begin{aligned} T_p(s) &= \frac{C_p(s) P_p(s)}{1 + C_p(s) P_p(s)} \\ &= \frac{\frac{C_{0p}(s)}{s}}{1 + \frac{C_{0p}(s)}{s}} P_{p1}(s) e^{-\hat{T}_d s} \end{aligned} \quad (2.41)$$

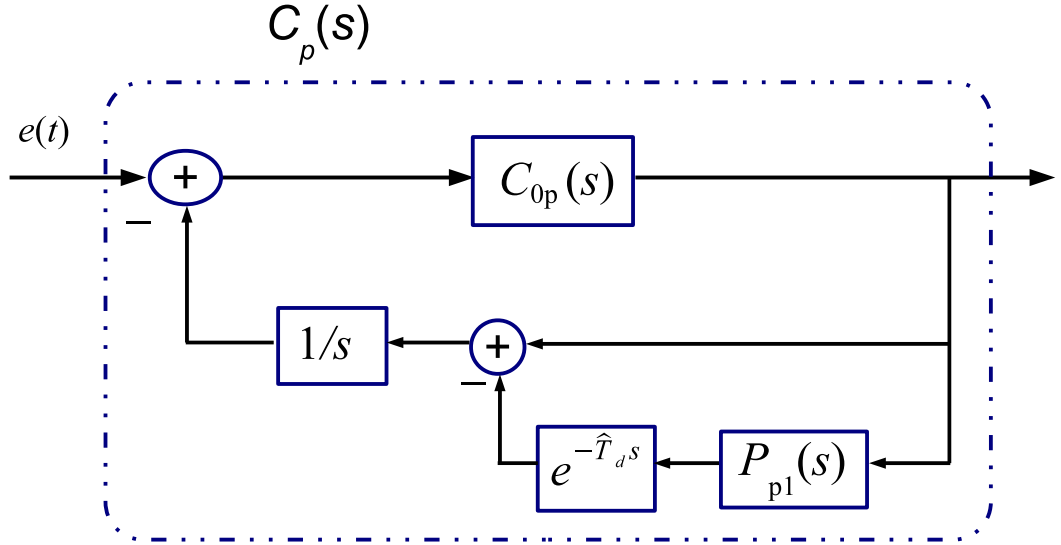


Figure 2.7: *Indirect approach for position control*

Stable P_{pl} does not affect the stability of the system. To ensure the stability of the feedback system, $C_{0p}(s)$ must stabilize the integrator. One of the structures proposed in Section 2.3 is used to complete controller design. Basically if we want $C_p(s)$ to include a pole at $s = 0$, we use the structure in Section 2.3.1 which offers C_{0p} as

$$C_{0p}(s) = \frac{(2p + p^2\hat{T}_d)s + p^2}{s - p^2\hat{T}_d}$$

where $p > 0$ is a free parameter chosen via Pole Placement Method. When we put $C_{0p}(s)$ into (2.41), the closed loop transfer function is obtained as

$$T_p(s) = \frac{((2p + p^2\hat{T}_d)s + p^2) ((2a + a^2\hat{T}_d)s + a^2)}{(s + p)^2 (s + a)^2} e^{-T_d s}$$

The poles of closed loop transfer functions are as same as the approach in Section 2.6.1. Only difference between the approaches is one of the zeros of the closed loop transfer function. Indirect approach also makes the controller design easier. Since the controller is designed for a plant which only includes integrator, we can utilize from the results in Section 2.3 directly. For position controller designs, we have used velocity controller $C_v(s)$ in Section 2.3.1. By using indirect approach, it is also simple to extend it to the other velocity controller designs.

Chapter 3

SIMULATIONS AND RESULTS

In this chapter, we will design examples of some controllers proposed in Section 3. These designs will be analyzed in terms of both robustness and performance. Performance is analyzed for both setpoint response and disturbance rejection. Robustness of the designed controller is also investigated for unmodeled dynamics and parametric uncertainty.

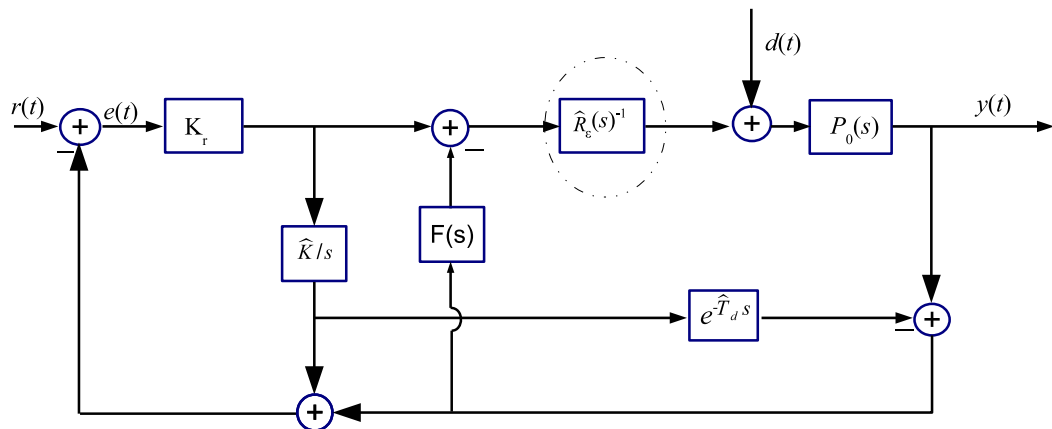


Figure 3.1: *The alternative Smith predictor based controller of Matausek and Micic*

Proposed controllers are compared with the alternative Smith predictor based controller of Matausek and Micic proposed in [17] which is proved to offer good

performance. This work is used in many other applications for comparison purposes. However, controller is designed only for integrative systems in [17]. In order to do a fair comparison, we will also use the inverse of the flexible modes in their controller structure as shown in Figure 3.1.

We will define a transfer function in the format of (2.2) arbitrarily for a robot arm. The plant taken into consideration is

$$P_0(s) = \frac{20}{s} R_0(s) e^{-0.2s} \quad (3.1)$$

where R_0 includes flexible modes

$$R_0(s) = \frac{\left(\frac{s}{\tilde{\omega}_1}\right)^2 + 2\frac{\tilde{\zeta}_1}{\tilde{\omega}_1}s + 1}{\left(\left(\frac{s}{\omega_1}\right)^2 + 2\frac{\zeta_1}{\omega_1}s + 1\right) \left(\left(\frac{s}{\omega_0}\right)^2 + 2\frac{\zeta_0}{\omega_0}s + 1\right)} \quad (3.2)$$

with the values $\tilde{\omega}_1 = 115$, $\tilde{\zeta}_1 = 0.22$, $\omega_1 = 125$, $\zeta_1 = 0.06$, $\omega_0 = 95$, $\zeta_0 = 0.15$.

We will propose different designs for this robot arm and compare the results with the one of Matausek and Micic.

3.1 Different Designs for Velocity Control

Two different design will be proposed. In controller design, we will assume that $P = P_0$, $\hat{K} = K$, $\hat{T}_d = T_d$, $\hat{R}_0 = R_0$ and $\varepsilon \rightarrow 0$. The effects of mismatch will be investigated in Section 3.3.

1. Firstly, an example of the design in Section 2.3.2 is proposed to reject constant and ramp disturbances. For the plant in (3.1), the chosen parameters are $a = 1.75$ and $e = 0.75$ that leads to $b = 3.68$, $c = 1.77$ and

$$C_{0v}(s) = \frac{5.433s^2 + 6.147s + 2.297}{s^2 - 1.183s - 0.4594}$$

Thus, we have $T_{ry}(s) = T_0(s)H(s)$ where

$$T_0(s) = \frac{5.433s^2 + 6.147s + 2.297}{(s + 1.75)^2 (s + 0.75)}$$

Normally, we choose $H(s)$ to eliminate the fastest real zero of $T_0(s)$. Since $T_0(s)$ has no real zero, we select $H(s) = (1 + s/0.5)^{-1}$ randomly in setpoint analysis.

2. Secondly, we will analyse the example of design proposed in Section 2.3.3. It will show us functionality of the controller for periodic disturbances with known frequency. We select the disturbance frequency $\omega_d = 1.5 \text{ rad/sn}$. Parameters of the controller are chosen as $a = 1$, $e = 2$ and $f = 3$. Corresponding controller is obtained as

$$C_{0v}(s) = \frac{5.117s^3 + 5.356s^2 + 8.6s + 3}{s^3 - 1.117s^2 + 2.644s - 0.6}$$

Closed loop transfer function turns into

$$T_0(s) = \frac{(s + 0.48)(5.117s^2 + 2.88s + 7.217)}{(s + 1)^2(s^2 + 2s + 3)}$$

Since $T_0(s)$ has a real zero at $s = -0.48$, we select $H(s) = (1 + s/0.48)^{-1}$ to eliminate this zero.

3.2 Performance Analysis

This section will be divided into two parts. Performance will be analyzed in terms of set-point response and then disturbance rejection. It is assumed that $P = P_0$, $\hat{K} = K$, $\hat{T}_d = T_d$, $\hat{R}_0 = R_0$ and $\varepsilon \rightarrow 0$ for nominal system performance analysis. The effects of mismatch in these parameters will be discussed in Section 3.3.

3.2.1 Setpoint Response Analysis

Responses of proposed controllers and the alternative Smith predictor controller design of [17] are given in Figure 3.2. The proposed controller in Section 2.3.3 in a faster response: %2 settling time of 5.1 sec. The settling time of the design in Section 2.3.3 and the alternative controller are 8.46 and 13.12 respectively. Since proposed controllers have free parameters, it is also possible to further optimize

the setpoint response. However, robustness of the system will diminish from the fact that there is trade-off between robustness and performance. Corresponding torque demands for step responses are shown in Figure 3.3.

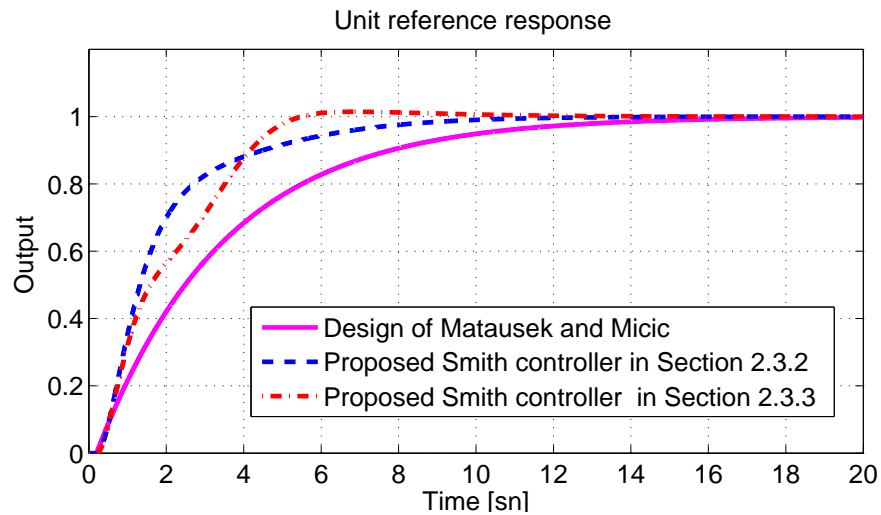


Figure 3.2: *Setpoint Responses*

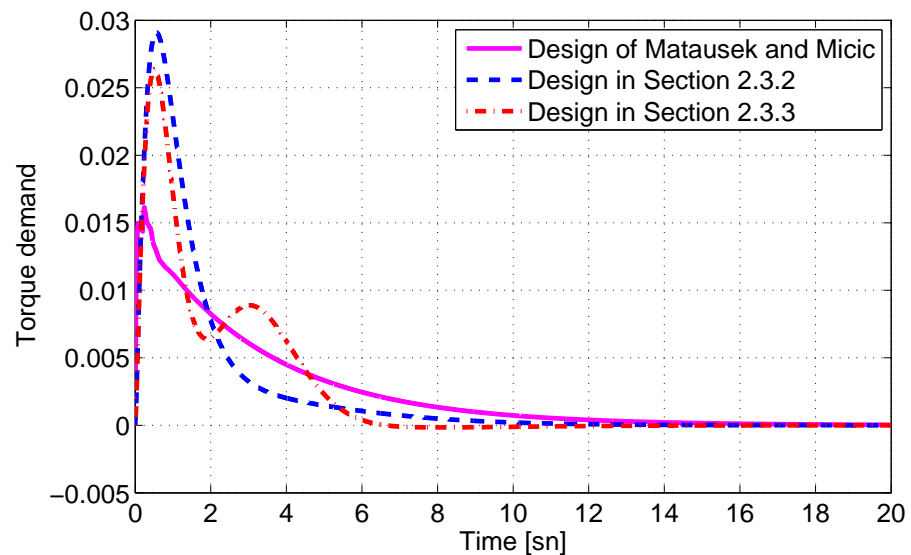


Figure 3.3: *Corresponding torque demands*

3.2.2 Disturbance Rejection

Disturbance rejection properties of the controllers are investigated by taking the transfer function between disturbance and output into consideration. If we define the velocity output as $y(t)$ and the disturbance as $d(t)$, the magnitude of this transfer function is defined as

$$|T_{yd}(j\omega)| = \left| \frac{P_0(j\omega)}{1 + P_0(j\omega)C_v(j\omega)} \right|$$

and the corresponding output magnitude is

$$|Y(j\omega)| = |T_{yd}(j\omega)| |D(j\omega)|.$$

To minimize the effect of disturbance, $|T_{yd}(j\omega)|$ is required to be as minimum as possible at the frequencies where the disturbance is dominant. Obtained results for the designs are shown in Figure 3.4.

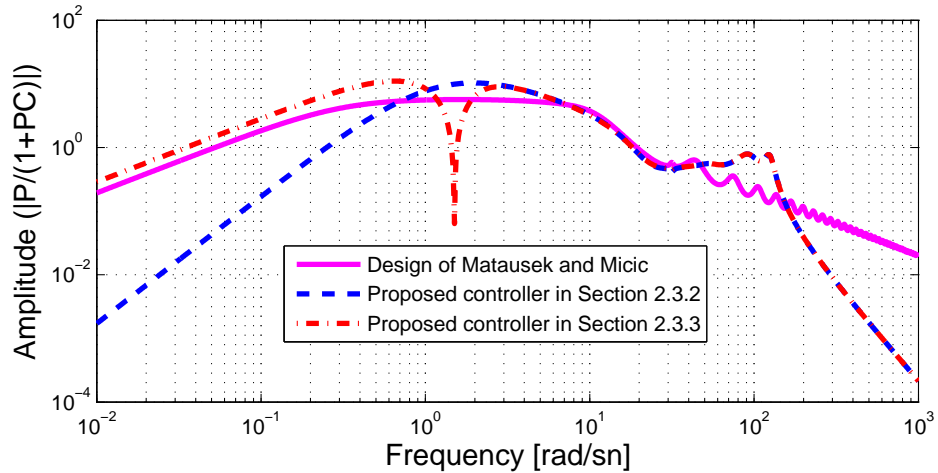


Figure 3.4: *Disturbance Rejection Property of The Controllers*

It is clear that the design in Section 2.3.2 results in fastest rejection for constant disturbance since it has two poles at $s = 0$. The design of Matausek and Micic and other proposed controller almost react in the same way against constant disturbance. By using two degree of freedom controller structure, Mataušek

and Micić, [17], provide satisfying disturbance rejection for constant load disturbances which is caused by derivative action and estimation of the disturbance signal. In the same manner, the effect of the design in Section 2.3.3 can be seen at the frequency of 1.5 rad/sn . It completely suppresses this sinusoidal signal. In addition to all, it is not possible to design a controller which is better than the others at all frequencies in terms of disturbance rejection. It is proven that while some advantages are gained at some frequencies, some performance is degraded at other frequencies. This is known as *waterbed effect* in the literature, [24]. Also designing a controller which suppresses constant and sinusoidal disturbance better than all is possible as indicated in Section 2.3.4. However, we will lose performance at other frequencies. It can be concluded that controller is preferred depending on design requirements.

3.3 Stability Robustness Analysis

Firstly, we will investigate stability margins of closed loop systems. For this purpose, open loop transfer function $G(j\omega)$ is analyzed:

$$\begin{aligned}
 G(s) &= P_0(s)C_v(s) \tag{3.3} \\
 &= \frac{K}{s}R_0(s)e^{-T_d s} \left(\frac{C_{0v}(s)}{1 + C_{0v}(s)\frac{(1-e^{-\hat{T}_d s})}{s}} \right) \frac{1}{\hat{K}}\hat{R}_\varepsilon^{-1}(s) \\
 &= \left(\frac{K}{\hat{K}} \right) (R_0(s)\hat{R}_\varepsilon^{-1}(s)) \frac{C_{0v}(s)e^{-T_d s}}{s + C_{0v}(s)(1 - e^{-\hat{T}_d s})}
 \end{aligned}$$

Let $\hat{T}_d = T_d$, $\hat{K} = K$ and define

$$G_0(s) = \frac{C_0(s)e^{-\hat{T}_d s}}{s + C_o(s)(1 - e^{-\hat{T}_d s})}.$$

The case $R_0(s)\hat{R}_\varepsilon^{-1}(s) \neq 1$ will be considered as dynamic uncertainty and discussed later at the end of this section.

The gain and phase margins obtained from Nyquist graph of $G_0(j\omega)$ give the information on how much uncertainty in the gain (K/\hat{K}) and delay mismatch

$(T_d - \widehat{T}_d)$ can be tolerated, [20]. The importance of phase margin emerges more in time-delayed system. Uncertainty in delay ΔT_d causes phase to be shifted as much as $e^{-\Delta T_d s}$. In this point, it is necessary to define maximum uncertainty in delay without damaging stability. It is called as delay margin [20] and can be shown as

$$DM = \frac{PM}{\omega_c}$$

where PM is phase margin and ω_c is gain crossover frequency. The best way to analyze the robustness in the presence of both gain and phase perturbation is the vector margin (VM), which is defined as the distance between the critical point, -1 , and $G_0(j\omega)$:

$$VM = \min_{\omega} |1 + G_0(j\omega)| \quad (3.4)$$

These values will determine the behaviour of the system under parametric uncertainties. Obtained Nyquist graphs for proposed designs are given in Figure 3.5 and 3.6.

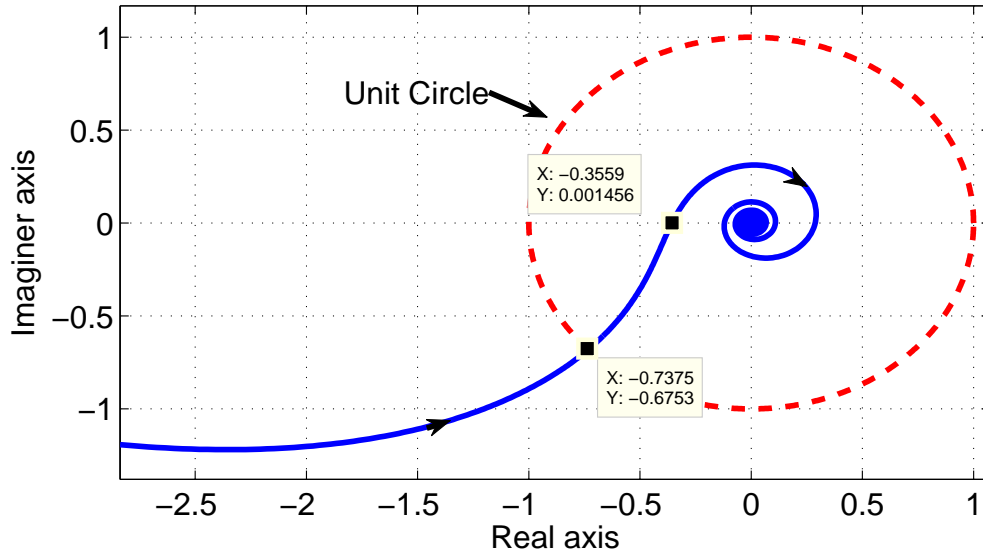


Figure 3.5: *Nyquist Graph For The Design in Section 2.3.2*

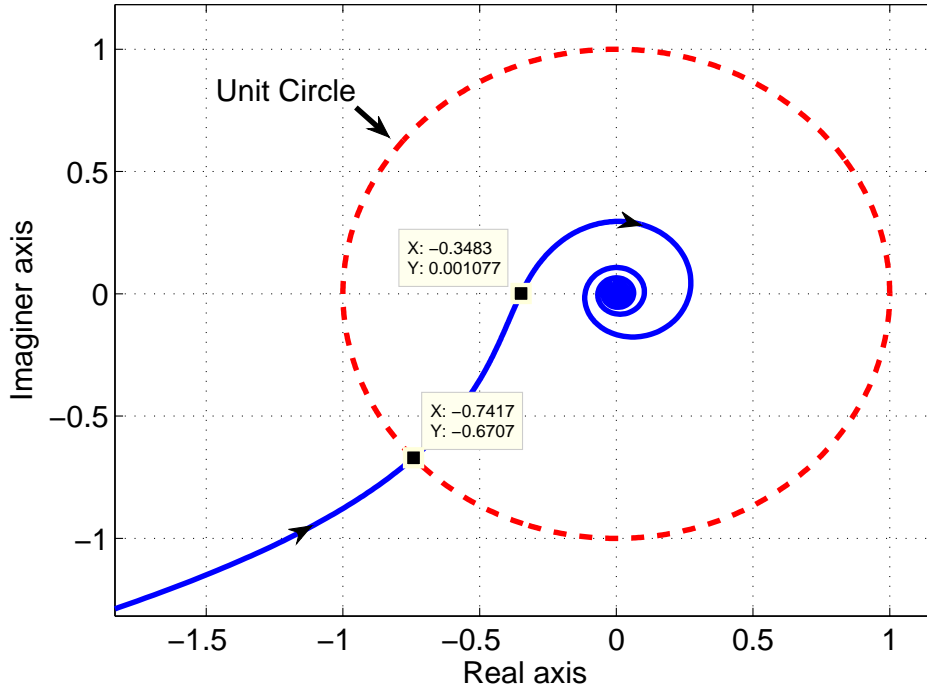


Figure 3.6: *Nyquist Graph For The Design in Section 2.3.3*

Corresponding stability margins are given in Table 3.1. It should be noted that, stability margins can be improved by changing free parameters. However, this may deteriorate the setpoint tracking and disturbance rejection performances. For the systems designed, VM is equal to 0.60 which is relatively large for good

Table 3.1: Stability Margins of The Designs

Controller Structure	GM	PM	VM	DM (sn)
The design of Matausek and Micic	2.23	57	0.53	0.25
Design in Section 2.3.2	2.81	43	0.60	0.26
Design in Section 2.3.3	2.87	42	0.60	0.24

stability robustness. Robustness to variations in the gain K and delay T_d is analyzed by calculating the VM when these parameters are fixed as $\hat{K} = 20$, $\hat{T}_d = 0.2$ sec in the controller but they are modified in the plant, taking values in the intervals $K \in [1, 60]$ and $T_d \in [0, 0.55]$ sec. The example for the design in

Section 2.3.3 can be seen in Fig. 3.7. This figure also shows the stability boundary (where $VM = 0$). We determine the point where $T_d - \hat{T}_d = 0$ and $K/\hat{K} = 1$ as the nominal operating point. If we move in x and y directions beginning from nominal operating point, maximum reachable points without damaging stability introduce us gain and delay margins respectively.

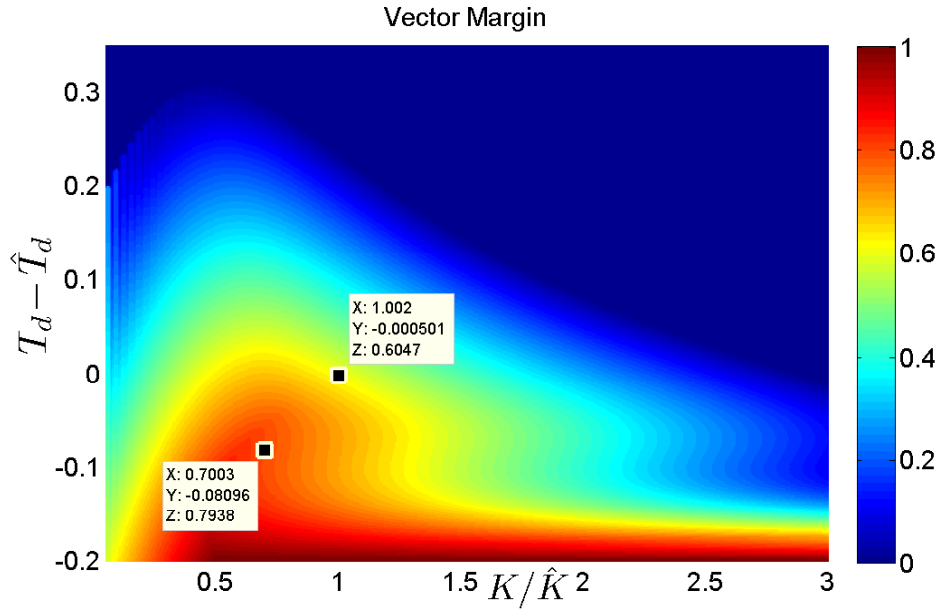


Figure 3.7: *Vector Margin For Different K and T_d*

In controller design, using Fig. 3.7 effectively can be very useful to increase robustness. For example, Fig. 3.7 shows that if the ratio (K/\hat{K}) is decreased to 0.7 (i.e. \hat{K} is chosen as 28.5) and the difference $T_d - \hat{T}_d$ is decreased to -0.08 (i.e. \hat{T}_d is chosen as 0.28), vector margin becomes 0.794. That also leads to increase in the other stability margins. With this modification, obtained setpoint responses and disturbance rejection properties are shown in Figure 3.8 and Figure 3.9 respectively.

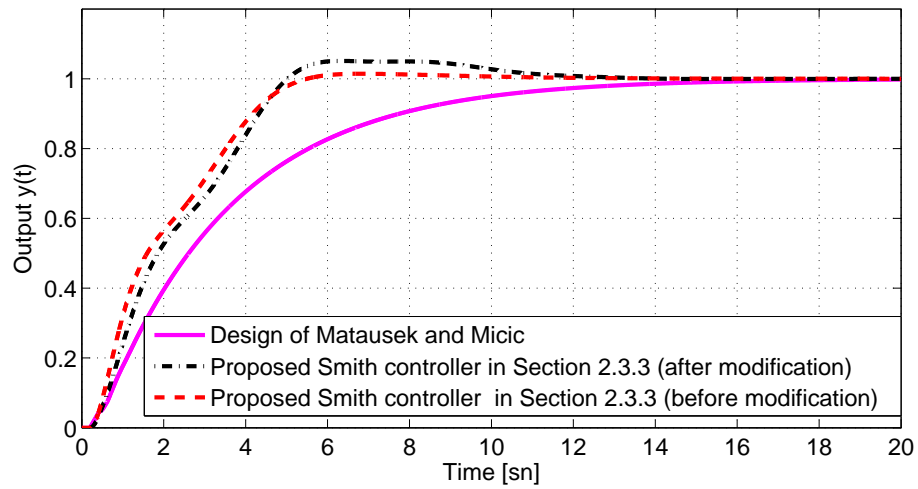


Figure 3.8: *Corresponding Step Responses*

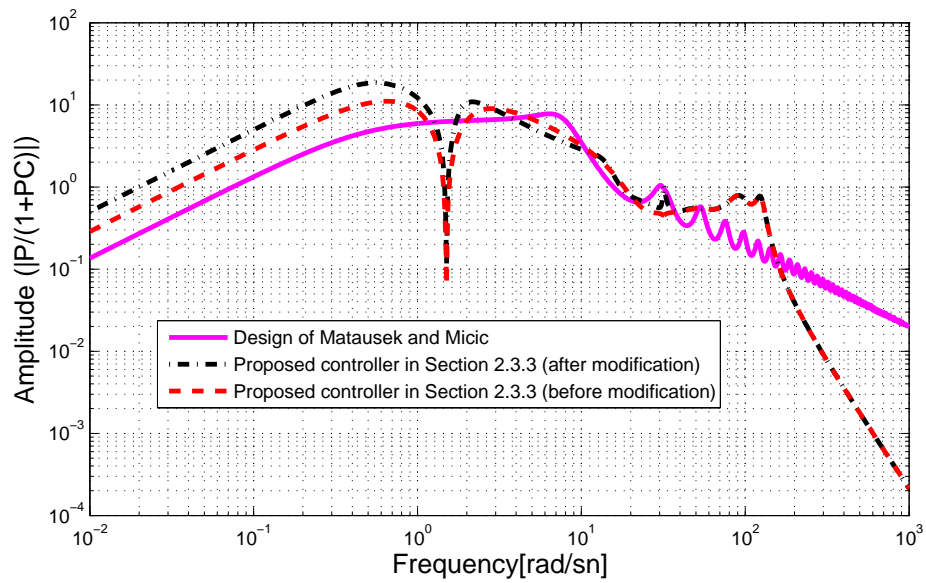


Figure 3.9: *Corresponding Disturbance Rejection Properties*

Figure 3.8 and Figure 3.9 show that better stability margins are obtained with the expense of slight performance loss. Such a performance loss is expected from the fact that there is a trade-off between robustness and performance levels, [24].

In order to analyze stability/robustness in the presence of dynamic uncertainty, consider the plant

$$P(s) = P_0(s)(1 + \Delta_m(s)) \quad (3.5)$$

where $\Delta_m(s)$ is multiplicative uncertainty, which is assumed to be stable.

The feedback system formed by the nominal controller designed as above and the uncertain plant (3.5) is robustly stable if and only if

$$|\Delta_m(j\omega)| < \frac{1}{|T_0(j\omega)|} \quad \forall \omega, \quad (3.6)$$

where $T_0(s)$ is closed loop transfer function. Recall that there are 8 parameters in the plant (3.1)–(3.2); varying each one of these will give a plant in the form (3.5), with a corresponding $\Delta_m(j\omega)$. Considering 20% variation in the nominal values of these 8 parameters we obtain a family of Δ_m . Fig. 3.10 shows that all of these $|\Delta_m(j\omega)|$ (red lines) remain below the graph of $1/|T_0(j\omega)|$ for proposed controllers. hence satisfying the robust stability inequality (3.6). Moreover, the gap between the red and blue lines represent how much *additional uncertainty* can be tolerated at each frequency. On the other hand, the benchmark controller of [17] shows an unstable response for combined perturbations for parameters.

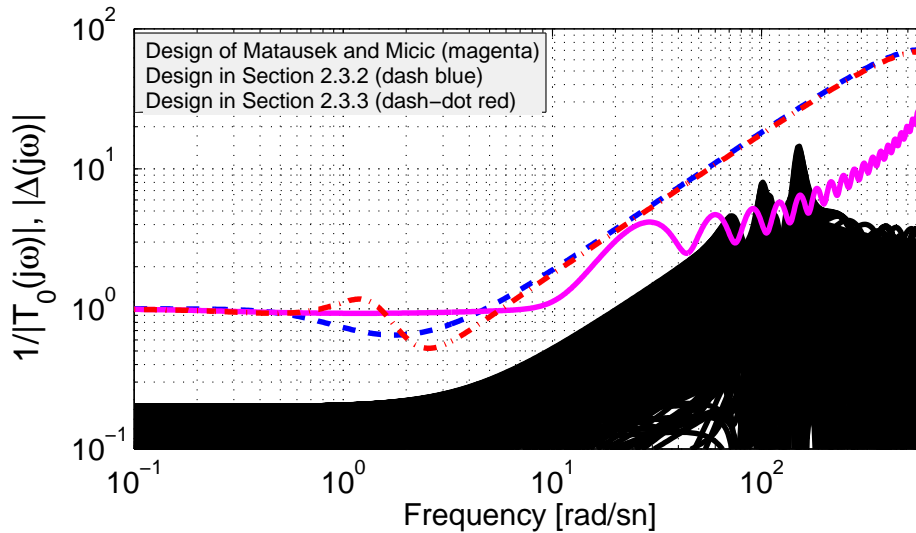


Figure 3.10: *Illustration of Robust Stability*

3.4 Examples For Position Control

In this section, we will demonstrate how the position controller is used. First of all, a velocity controller is designed to obtain $C_v(s)$ shown in Figure 2.5. It will be in the structure of proposed controller in Section 2.3.1 which behaves like a PI controller. By choosing simply $a = 1$, internal controller is

$$C_{0v} = \frac{2.2s + 1}{s - 0.2}$$

Then, position controller C_p can be designed in two ways as proposed. Firstly, the controller is designed in direct approach to stabilize

$$P_p = \frac{2.2s + 1}{s(s + a)^2} e^{-T_d s}.$$

Here $P_{p1} = \frac{2.2s + 1}{(s + a)^2}$ is delay-free part of closed loop transfer function of velocity control system. By choosing $p = 30$, designed internal controller for position loop is

$$C_{0p} = \frac{132s^2 + 2940s + 900}{s^3 + 62s^2 + 889s - 180}.$$

Secondly, we will show the structure of the controller by using indirect approach. Internal controller C_{0p} is designed to stabilize integrator like velocity controller. When we choose $p = 5$, obtained controller is

$$C_{0p} = \frac{15s + 25}{s - 5}.$$

Corresponding unit step responses for these designs are shown in Figure 3.11 and 3.12 respectively. In these designs, a reference filter with cut-off frequency of 1 rad/sn is used to develop tracking response.

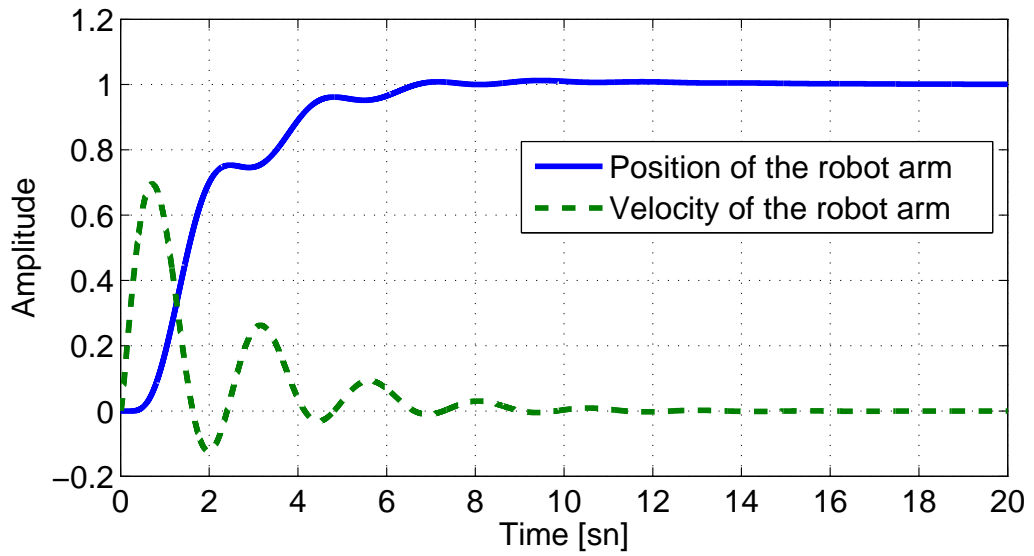


Figure 3.11: *Unit step response for direct approach*

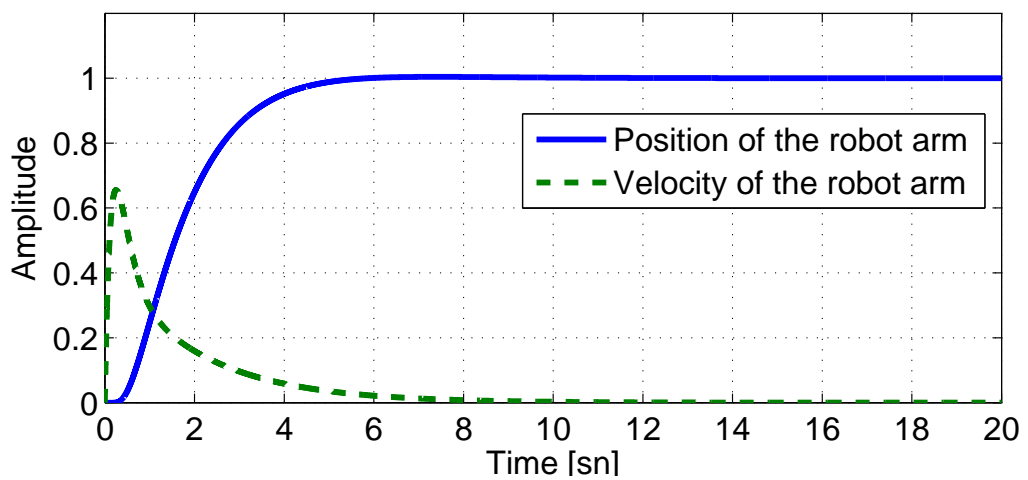


Figure 3.12: *Unit step response for indirect approach*

It is also possible to design these controllers with other parameters. However, we need to pay attention to velocity demand of position controller. Acceleration limit of the motor cannot be enough to satisfy the demand in designated time. For comparison, indirect approach seems more practical to be used in terms of both

simplicity and system response. Also it is necessary to investigate the response of the systems under some parametric uncertainties in the plant. For %20 deviation on time delay, the corresponding responses are given in Figure 3.13. The results show the effectiveness of the hierarchical structure and designed controllers under time delay uncertainty.

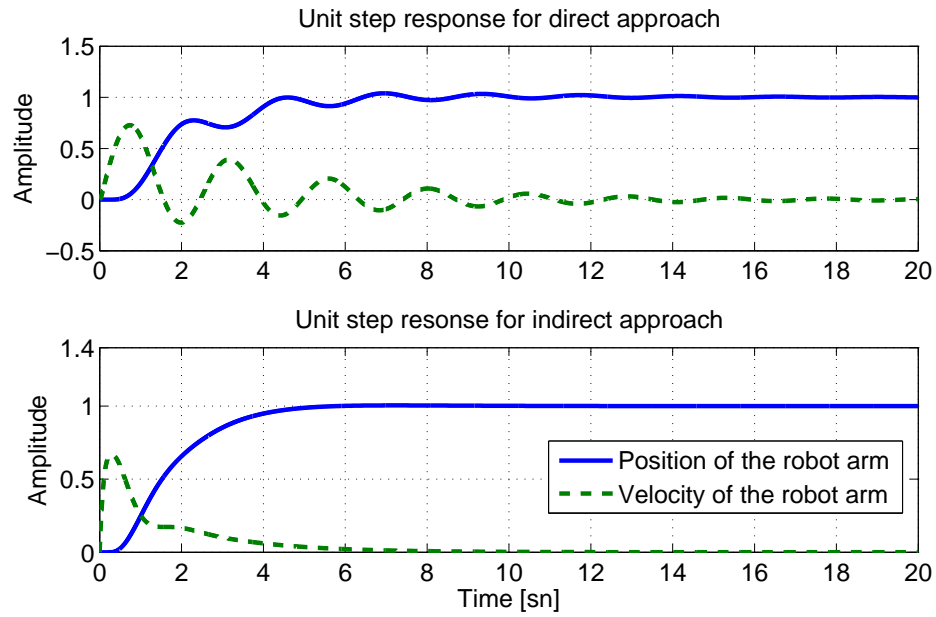


Figure 3.13: *Unit step response for %20 deviation on time delay T_d*

In addition to all, the step responses are also analyzed under %20 of perturbation for all parameters of flexible modes. While damping ratios are decreased by %20, damping frequencies are increased by %20. It seen from Figure 3.14 that the results are not much different from nominal case.

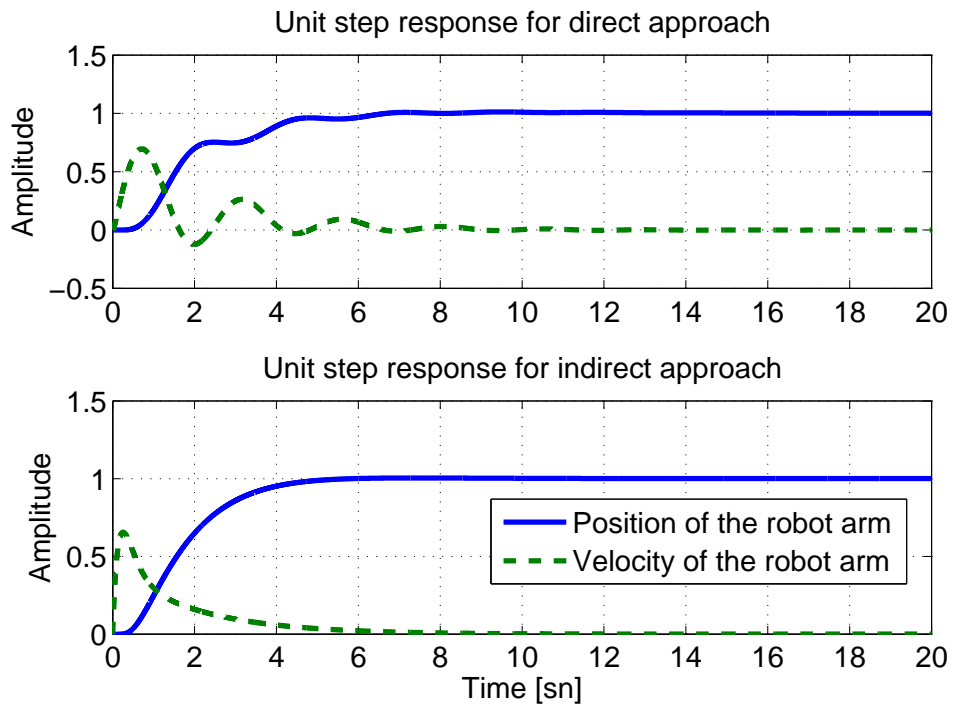


Figure 3.14: *Unit step response for 20% perturbation on the parameters of flexible modes*

Chapter 4

CONCLUSIONS

In this thesis, a Smith predictor based controller structure is considered for a flexible robot arm. Based on interpolation conditions imposed by constant, ramp and periodic disturbance rejection, the free part of the controller, $C_{0v}(s)$ is designed. The order of resulting $C_{0v}(s)$ changes depending on the structure of the controller. Free parameters of the designs determine the closed loop system pole locations. Optimization of these parameters for other performance and robustness measures is possible.

A first order low-pass filter is used to filter the reference signal. Usage of this filter does not affect disturbance attenuation, but it improves tracking response. We determine the cut-off frequency of the filter depending on the requirements on the system overshoot and settling time. Also, Pade approximation is used to remove delay term in controller. In this way, we can see the structure of the overall controller clearly.

By using the hierarchical control structure, another Smith predictor based controller is designed for the position loop. After the design of velocity controller, position controller is designed by using closed loop transfer function of velocity control system. Two different approaches are proposed for this purpose. They use similar structure, however the internal controllers C_{0p} stabilizes different transfer functions.

In the implementation of the overall controller $C_v(s)$, shown in Fig. 2.2, the feedback loop around C_{0v} is a filter whose impulse response is finite duration $\frac{1 - e^{-\hat{T}_d s}}{s}$. So, this component can be implemented easily in a numerically reliable manner. The controller also uses the (approximate) inverse of the stable minimum phase part of the plant, $1/(K\hat{R}_\varepsilon(s))$. Robustness to uncertainties in K , T_d and the parameters of $R_0(s)$ are also demonstrated. If an upper bound of multiplicative uncertainty is given, then it is possible to use H_∞ control techniques to modify the design of C_0 accordingly.

Bibliography

- [1] E. J. Adam, H.A. Latchman, and O.D. Crisalle. Robustness of the Smith predictor with respect to uncertainty in the time-delay parameter. In *American Control Conference, 2000. Proceedings of the 2000*, volume 2, pages 1452–1457 vol.2, 2000.
- [2] K.J. Aström and T. Hägglund. *PID Controllers: Theory, Design, and Tuning*. Instrument Society of America, 1995.
- [3] K.J. Aström, C.C Hang, and B. C. Lim. A new Smith predictor for controlling a process with an integrator and long dead-time. *Automatic Control, IEEE Transactions on*, 39(2):343–345, 1994.
- [4] G. R. Chen, A. Desages, and P. Julian. Trajectory tracking and robust stability for a class of time-delayed flexible-joint robotic manipulators. *International Journal of Control*, 68(2):259–276, 1997.
- [5] L. De Cicco, S. Mascolo, and S. I. Niculescu. Robust stability analysis of Smith predictor-based congestion control algorithms for computer networks. *Automatica*, 47(8):1685 – 1692, 2011.
- [6] B.A. Francis and W.M. Wonham. The internal model principle of control theory. *Automatica*, 12(5):457 – 465, 1976.
- [7] K.S Fu, R. C. Gonzalez, and C. S. George Lee. *Robotics: control, sensing, vision, and intelligence*. McGraw-Hill, 1987.

- [8] J.L. Guzman *et al.* Interactive tool for analysis of time-delay systems with dead-time compensators. *Control Engineering Practice*, 16(7):824 – 835, 2008.
- [9] K. S Hong and D. H. Kang. Reclaimer control: modeling, identification, and a robust Smith predictor. In *Intelligent Robots and Systems, 1999. IROS '99. Proceedings. 1999 IEEE/RSJ International Conference on*, volume 1, pages 344–349 vol.1, 1999.
- [10] B. Kristiansson and B. Lennartson. Robust PI and PID controllers including Smith predictor structure. In *American Control Conference, 2001. Proceedings of the 2001*, volume 3, pages 2197–2202 vol.3, 2001.
- [11] D. L. Laughlin, D. E. Rivera, and M. Morari. Smith predictor design for robust performance. *International Journal of Control*, 46(2):477–504, 1987.
- [12] D. Lee, M. Lee, S. Sung, and I. Lee. Robust PID tuning for Smith predictor in the presence of model uncertainty. *Journal of Process Control*, 9(1):79 – 85, 1999.
- [13] K. Lee, B., Chen H. W., and B. S. Chen. Power control of cellular radio systems via robust Smith prediction filter. *Wireless Communications, IEEE Transactions on*, 3(5):1822–1831, 2004.
- [14] S. Majhi and D. P. Atherton. Obtaining controller parameters for a new Smith predictor using autotuning. *Automatica*, 36(11):1651 – 1658, 2000.
- [15] S. Mascolo. Congestion control in high-speed communication networks using the Smith principle. *Automatica*, 35(12):1921 – 1935, 1999.
- [16] M. R. Mataušek and A. D. Micić. A modified Smith predictor for controlling a process with an integrator and long dead-time. *Automatic Control, IEEE Transactions on*, 41(8):1199–1203, 1996.
- [17] M. R. Mataušek and A. D. Micić. On the modified Smith predictor for controlling a process with an integrator and long dead-time. *Automatic Control, IEEE Transactions on*, 44(8):1603–1606, 1999.

- [18] C. I. Morrescu, S. I. Niculescu, and K. Gu. On the geometry of stability regions of Smith predictors subject to delay uncertainty. *IMA Journal of Mathematical Control and Information*, 24(3):411–423, 2007.
- [19] J.E. Normey-Rico and E.F. Camacho. Robust tuning of dead-time compensators for processes with an integrator and long dead-time. *Automatic Control, IEEE Transactions on*, 44(8):1597–1603, 1999.
- [20] H. Ozbay. *Introduction to Feedback Control Theory*. CRC Press, Inc., Boca Raton, FL, USA, 2000.
- [21] R. Sipahi, S.-I. Niculescu, C.T. Abdallah, W. Michiels, and Keqin Gu. Stability and stabilization of systems with time delay. *Control Systems, IEEE*, 31(1):38–65, 2011.
- [22] O. J. M. Smith. Closer control of loops with dead time. *Chemical Engineering Progress*, 53:217–219, 1957.
- [23] M. W. Spong, S. Hutchinson, and M. Vidyasagar. *Robot modeling and control*. John Wiley & Sons, Inc., New York,, 2006.
- [24] G. Stein. Respect the unstable. *Control Systems, IEEE*, 23(4):12–25, 2003.
- [25] P. Van der Smagt and G. Hirzinger. The cerebellum as computed torque model. In *Knowledge-Based Intelligent Engineering Systems and Allied Technologies, 2000. Proceedings. Fourth International Conference on*, volume 2, pages 760–763 vol.2, 2000.
- [26] A. Visioli and Q-C. Zhong. *Control of Integral Processes with Dead Time*. Springer, 2011.
- [27] K. Watanabe and M. Ito. A process-model control for linear systems with delay. *Automatic Control, IEEE Transactions on*, 26(6):1261–1269, 1981.
- [28] D.C. Youla, H. Jabr, and J. J. Bongiorno. Modern wiener-hopf design of optimal controllers—part ii: The multivariable case. *Automatic Control, IEEE Transactions on*, 21(3):319–338, 1976.